

# Contribution of fluorescent primary biological aerosol particles to low-level Arctic cloud residuals

Gabriel Pereira Freitas<sup>1,2</sup>, Ben Kopec<sup>3</sup>, Kouji Adachi<sup>4</sup>, Radovan Krejci<sup>1,2</sup>, Dominic Heslin-Rees<sup>1,2</sup>, Karl Espen Yttri<sup>5</sup>, Alun Hubbard<sup>6,7</sup>, Jeffrey M. Welker<sup>8,9,10</sup>, and Paul Zieger<sup>1,2</sup>

<sup>1</sup>Department of Environmental Science, Stockholm University, Stockholm, Sweden

<sup>2</sup>Bolin Centre for Climate Research, Stockholm University, Stockholm, Sweden

<sup>3</sup>Great Lakes Research Center, Michigan Technological University, Houghton, USA

<sup>4</sup>Department of Atmosphere, Ocean, and Earth System Modeling Research, Meteorological Research Institute, Tsukuba, Japan

<sup>5</sup>The Climate and Environmental Research Institute NILU, Kjeller, Norway

<sup>6</sup>IC3 - Centre for Ice, Cryosphere, Carbon and Climate, Institutt for Geovitenskap, UiT - The Arctic University of Norway, Tromsø, Norway

<sup>7</sup>Geography Research Unit, University of Oulu, Oulu, Finland.

<sup>8</sup>Department of Biological Sciences, University of Alaska Anchorage, Anchorage, USA

<sup>9</sup>University of the Arctic, Rovaniemi, Finland

<sup>10</sup>Ecology and Genetics Research Unit, University of Oulu, Oulu, Finland

**Correspondence:** Paul Zieger (paul.zieger@aces.su.se)

**Abstract.** Mixed-phase clouds (MPC) are key players in the Arctic climate system due to their role in modulating solar and terrestrial radiation. Such radiative interactions ~~critically rely~~ rely, among other factors, on the ice content of MPC which ~~;~~ in turn, also depend on is regulated by the availability of ice nucleating particles (INP). ~~INP sources and concentrations are poorly understood in the Arctic. Recently, INP active at high temperatures were~~ While it appears that INP are associated with the presence of primary biological aerosol particles (PBAP) in the Arctic, the nuances of the processes and patterns of INP and their association with clouds and moisture sources have not been resolved. Here, we investigated for a full year the abundance and variability of fluorescent PBAP (fPBAP) within cloud residuals, directly sampled by a multiparameter bioaerosol spectrometer coupled to a ground-based counterflow virtual impactor inlet at the Zeppelin Observatory (475 m asl), Ny-Ålesund, Svalbard. fPBAP concentrations ( $10^{-3}$ – $10^{-2}$  L<sup>-1</sup>) and contributions to coarse-mode ~~aerosol~~ cloud residuals (0.1 to 1 in every  $10^3$  particles) ~~within cloud residuals~~ were found to be close to those expected for ~~concentrations of~~ high-temperature INP. Transmission electron microscopy ~~also~~ confirmed the presence of PBAP, most likely bacteria, within ~~the cloud residual samples~~ one cloud residual sample. Seasonally, our results reveal an elevated presence of fPBAP ~~within~~ cloud residuals in summer. Parallel water vapor isotope measurements point towards a link between summer clouds and regionally sourced air masses. Low-level MPC were predominantly observed at the beginning and end of summer, and one explanation for their presence is the existence of high-temperature INP. In this study, we present direct observational evidence that fPBAP may play an important role in determining the phase of low-level Arctic clouds. These findings have potential implications for the future description of sources of ~~cloud condensation ice~~ nuclei given ongoing changes in the hydrological and biogeochemical cycles that will influence the PBAP flux in and towards the Arctic.

## 1 Introduction

20 Mixed phase clouds (MPC) contain both cloud droplets and ice crystals (Korolev et al., 2003). Their interaction with solar and terrestrial radiation depends on their ice-to-droplet ~~mixing-ratio~~, altitude, thickness and other factors (Matus and L'Ecuyer, 2017). The phase of an MPC ~~is-can be~~ affected by the aerosol population in the cloud (Storelvmo, 2017), especially by the presence of particles that can facilitate the formation of ice ~~within the cloud~~, the ice nucleating particles (INP; see e.g. Kanji et al., 2017). Therefore, a key element in an improved understanding of MPC in the Arctic is unraveling the sources, properties  
25 and concentrations of INP (Solomon et al., 2018).

The representation of MPC and other aerosol-cloud interactions are important sources of uncertainties in climate models, impacting our ability to correctly estimate radiative forcing in the Earth's climate system (Szopa et al., 2021). This is especially true in remote regions, such as the Arctic, where measurements are scarce (Schmale et al., 2021) and low-level MPC are prevalent throughout the year (Kay et al., 2016; Morrison et al., 2012). The Arctic has experienced surface temperature increases  
30 that are two to four times higher than the global average (Rantanen et al., 2022), a phenomenon known as Arctic amplification (Wendisch et al., 2023). Clouds are believed to be ~~one-a~~ key contributor to the Arctic radiative budget, prompting the need to improve our understanding of aerosol-cloud interactions in the Arctic (Schmale et al., 2021).

INP facilitate ice growth at temperatures above that of homogeneous nucleation (temperatures below  $-38^{\circ}\text{C}$ , Kanji et al., 2017). Complete or partial glaciation of a cloud radically changes its radiative properties and lifetime and can even trigger  
35 precipitation (Lensky and Rosenfeld, 2003; Stopelli et al., 2015). In the Arctic, ~~high-temperature~~ high-temperature INP have been observed on a seasonal basis (Porter et al., 2022; Sze et al., 2023) and have been linked to biogenic oceanic and terrestrial sources (~~Šantl-Temkiv et al., 2019; Hartmann et al., 2020; Pereira Freitas et al., 2023~~) (Creamean et al., 2018; Šantl-Temkiv et al., 2019; F  
along with dust emissions (Tobo et al., 2019). Satellite observations show that the prevalence of MPC in the Arctic and Antarctic regions can be explained to a large degree by the presence of INP (Carlsen and David, 2022). Despite satellite remote  
40 sensing uncertainties, their results reflect those of ground-based remote sensing in the Arctic (Nomokonova et al., 2019).

Primary biological aerosol particles (PBAP) are biological particles that are emitted directly from the source to the atmosphere. These can be, but are not limited to, microorganisms, biological functional parts, fungal spores or ~~just~~ fragments of  
vegetation (Després et al., 2012; Fröhlich-Nowoisky et al., 2016). Some PBAP are efficient INP, even at high temperatures ( $>-15^{\circ}\text{C}$ , Tobo et al., 2013). This is due to their microphysical properties and/or their excretion of ice nucleating proteins (Pummer  
45 et al., 2015). In the Arctic, PBAP dominate the number of high-temperature INP in summer (Sze et al., 2023; Pereira Freitas et al., 2023).

Some PBAP, such as bacteria, have been observed in cloud water samples ~~that and~~ showed cloud condensation (Bauer et al., 2002, 2003) and ice nucleating abilities (Joly et al., 2013). These in-cloud bacteria undergo cloud processing (Khaled et al., 2021), reproduction and growth (Sattler et al., 2001). ~~The offline~~ Offline methods used to sample ~~bacteria, however,~~ PBAP are  
50 limited in quantifying ~~the abundance of PBAP~~ their abundance (Huffman et al., 2020). To overcome such limitations, online methods can be used, such as those based on single-particle ultraviolet laser-induced fluorescence (Huffman et al., 2020), which have been shown to give reasonable estimates of PBAP concentration in real time (Freitas et al., 2022; Crawford et al.,

2017, 2020). Given the close link between PBAP and high-temperature INP (Šantl-Temkiv et al., 2019; Creamean et al., 2019; Pereira Freitas et al., 2023), obtaining PBAP concentrations inside cloud particles is one way to understand the impact of PBAP serving as INP in cloud glaciation.

The ground-based counterflow virtual impactor (CVI) has been successfully used in recent years to improve our process-level understanding of aerosol-cloud interactions in the Arctic, for example, by determining the size distributions (of sub-micrometer aerosol, Karlsson et al. (2021, 2022)), the chemical composition (Gramlich et al., 2023) or the black carbon concentration (Zieger et al., 2023) of cloud residuals, i.e. particles which were involved in cloud formation or cloud processes. In this study, we present the first investigation of the contribution of PBAP to cloud residuals in the Arctic.

Some studies ~~link INP or PBAP to local and regional sources (Pereira Freitas et al., 2023; Creamean et al., 2022) or transportation from lower latitudes (Meinander et al., 2022; Shi et al., 2022; Si et al., 2019)~~ evaluated the sources of INP and PBAP by using back trajectories ~~as a tool to investigate air mass origin and to identify potential source areas (Si et al., 2019; Meinander et al., 2022; Shi et al., 2022)~~. Another method to investigate the air origin is to use the water isotope ratios (hydrogen,  $\delta D$  and oxygen,  $\delta^{18}O$ ), which has been used to distinguish ~~local~~ regional and transported sources of air (Sodemann et al., 2008; Sjoström and Welker, 2009; Bonne et al., 2015; Noone et al., 2011). This determination of source and transport history is possible because ~~deuterium excess isotope ratios~~ in water vapor and precipitation is largely controlled by the conditions at the point of evaporation ~~(Merlivat and Jouzel, 1979)~~ , which changes as the air mass is carried over the atmosphere (Merlivat and Jouzel, 1979; Xia et al., 2022). In the Arctic, water isotopic measurements have been used to distinguish between moisture sourced ~~locally~~ regionally, in response to variations in sea ice coverage, and moisture sourced from distant locations (Kopeck et al., 2016; Bonne et al., 2019; Akers et al., 2020; Bailey et al., 2021). In Svalbard, ~~the site of interest of this study, and among other locations,~~ it has been shown that low deuterium ( $^2H$ ) excess values ( $< 5\text{‰}$ ) are typically driven by air masses comprised of predominantly ~~locally-sourced~~ regionally-sourced moisture while high ~~deuterium excess~~ values ( $> 10\text{‰}$ ) are found in air masses comprised of predominantly distant-sourced moisture (Kopeck et al., 2016). Pairing CVI ~~measurements of cloud residuals~~ sampling of cloud particles with water vapor isotopic measurements can ~~thus be used to better understand the~~ improve the understanding on the origin of a given air mass and aid in the source identification of INP and PBAP.

We investigate the presence and impact of PBAP in low-level Arctic clouds present at the Zeppelin Observatory, Svalbard, and address the following research questions: (i) Can we identify PBAP within cloud particles of low-level Arctic clouds using an online single-particle instrument coupled to a CVI inlet? (ii) If so, to what extent are they present throughout the year and what are their respective sources? And finally, (iii) if present, can we identify an impact on the cloud phase?

## 2 Methods

### 2.1 Campaign description

The measurements were part of the Ny-Ålesund Aerosol Cloud Experiment (NASCENT) 2019-2020 campaign. A complete overview of the campaign is given by Pasquier et al. (2022). In short, for one year and a half, which coincided with the MOSAiC expedition in the central Arctic (Shupe et al., 2022), several state-of-the-art aerosol, cloud and meteorological measurements

from different platforms were taken concurrently at various locations around Ny-Ålesund in a combined effort to unravel the properties of clouds and aerosols in the Arctic. In this work, we focus on measurements taken at the Zeppelin Observatory located 475 meters above sea level (asl) close to the top of the Zeppelin mountain, 2 kilometers south of the village (Pasquier et al., 2022). Due to the topography of the mountain, the wind tends to blow predominantly from the south or from the north, with very little influence from crosswinds (see e.g., Pasquier et al., 2022). The observatory was engulfed in low-level clouds for an extensive period 34% of the campaign (approx. 34%, when the visibility was duration (visibility) below 1 km as measured by the visibility sensor, see next section section 2.2). The entire setup is illustrated in Figure 1.

## 2.2 Cloud particle sampling

Cloud droplets and ice crystals were sampled collected using a ground-based counterflow virtual impactor (CVI) inlet (Brechtel Inc., USA, Model 1205). The CVI only samples larger particles (collects particles above approx.  $6 \mu\text{m}$  in aerodynamic diameter), representing aerosol particles that have been activated into cloud droplets or ice crystals. It does so by applying a counterflow accelerating the cloud onto the CVI tip that is installed within a wind tunnel. Within the CVI tip a counterflow is targeted against the sample flow, which where only larger particles have enough inertia to penetrate through the virtual impaction plate. A more technical description of the CVI is given in Noone et al. (1988); Shingler et al. (2012) and Noone et al. (1988) and Shingler et al. (2012), whereas a detailed characterization of the ground-based CVI present at the Zeppelin Observatory, together with the corrections that need to be applied applied corrections, is given in Karlsson et al. (2021). In summary, the measured concentrations of the cloud residuals After the cloud droplets and ice crystal penetrate through virtual impaction plate, they are dried in the counterflow air. The leftover nuclei are called cloud residuals, which are then sampled by the aerosol instrumentation downstream of the CVI. The measured cloud residual concentration after correcting for an enrichment factor have to (9.8 for this work) must be multiplied by a factor of 2, to account accounting for a mean droplet sampling efficiency of around 4845 %. This factor was determined by comparing the coarse-mode cloud residual particle concentration ( $> 0.8 \mu\text{m}$ ) measured by the MBS during the CVI operation with the corresponding ambient (total) coarse-mode particle concentration measured by a FIDAS 200S (Palas GmbH, Germany) sampling from its own inlet located on the terrace of Zeppelin observatory (see Fig. the Zeppelin Observatory (see Figure S1 in the SI). This value compares remarkably well with is comparable to the CVI sampling efficiency of 46 % previously determined by Karlsson et al. (2021) using the comparison of CVI observations with cloud microphysical measurements and the comparison of the aerosol size distribution of ambient and cloud residual accumulation mode measurements. After the cloud droplets and ice crystal penetrate through virtual impaction, they are dried in the counterflow air. Possible sampling artifacts, such as crystal shattering or particle capture by the wake effect, are discussed in detail in Karlsson et al. (2021). However, these artifacts that increase the number of particles are shown to be limited to particles in the Aitken mode (particles  $< 100 \text{ nm}$ ) and not the coarse mode, which is the focus size range of this work. In addition, coarse mode particles are commonly of primary origin; thus, it is likely that no major CVI sampling artifacts significantly influenced the results presented here.

A visibility sensor is was coupled to the CVI inlet (Belfort Instrument, USA, Model 6400). Whenever the visibility falls below 1000 meters, indicating the presence of clouds according to the WMO (Spänkuch et al., 2022; WMO, 2008), the CVI

120 inlet is meant to be turned on. For part of the observational period of this study, the CVI was turned on automatically. How-  
ever, for certain periods due to severe icing conditions, it was turned on manually. Given the manual operation of the CVI  
inlet and fluctuation of visibility to values above 1 km (leading to a short automatic stop of the CVI inlet sampling) within  
a short period, several cloud events (CE) could be contained within a single cloud, and some clouds were not sampled at  
all. Despite our best efforts to obtain a balanced data set throughout all seasons, the issues with icing on the inlet during  
125 cold periods with supercooled liquid cloud droplets led to fewer samples in the winter months. It should be noted that the  
summer generally shows denser clouds with a higher cloud water content and lower visibilities during cloudy conditions  
(see Fig. S6 in Zieger et al., 2023). However (see Figure S6 in Zieger et al., 2023). Nonetheless, there are several CE success-  
fully sampled during winter, thus covering all months of the year. The exception is April 2020, when the MBS did not function.  
An overview of the CE sampled is given in Table S1 (in the Supplementary Information, SI). The first minute of every CE was  
130 discarded to remove possible contamination by particles remaining in the inlet from previous sampling and switching of the  
inlet.

### 2.3 Single-particle bioaerosol characterization

The single particle characterization of the cloud residuals ~~is was~~ performed using a multiparameter bioaerosol spectrom-  
eter (MBS, University of Hertfordshire, U.K.). The MBS is a single-particle instrument based on ~~ultraviolet-light-induced~~  
135 ~~fluorescence~~. ~~A more complete description of the instrument is given by Ruske et al. (2017).~~ ~~laser-induced fluorescence~~  
(Ruske et al., 2017). In summary, ~~for our instrument,~~ a laminar sample flow ( $0.315 \text{ lpm L min}^{-1}$ ) shielded by a sheath flow  
( $1.715 \text{ lpm}$ , ~~leading to a~~  $\text{L min}^{-1}$ ,  $2.03 \text{ lpm}$  ~~as a~~  $\text{L min}^{-1}$  total flow) guides particles through the instrument. A continuous  
low-power laser ~~scatters light off of~~ ~~light is scattered by~~ particles, and their size is retrieved by the intensity of the scattered  
light. ~~Then, a xenon flashlamp is triggered shining at the particle with a 280 nm ultraviolet light.~~ The instrument can reli-  
140 ably measure the fluorescence of particles with an optical diameter of  $0.8 \mu\text{m}$  or larger. ~~Then, a xenon flashlamp is triggered~~  
~~shining at the particle with a 280 nm ultraviolet light.~~ If the particle fluoresces, its emitted light is collected by two collection  
mirrors and focused onto a diffraction grating. The diffracted light is then focused onto a detector covering the visible range  
between the wavelengths of 300-615 nm over 8 equally distant channels. Following the previous work by Freitas et al. (2022),  
if the fluorescence is more than 9 times the fluorescence background and its main signal sits at 364 nm (tryptophan emission  
145 channel, a common protein in microorganisms, see e.g. Pöhlker et al., 2012), the particle is classified as a fluorescent primary  
biological aerosol particle (fPBAP). A general drawback of ~~using ultra-violet laser-induced fluorescence (UV-LIF) as the main~~  
~~classification method these methods~~ are uncertainties relating to over-counting (fluorescent particles erroneously classified as  
PBAP) and under-counting (potential non-fluorescent PBAP ~~generally~~ not being counted).

### 2.4 Water vapor isotope measurements

150 Continuous atmospheric water vapor isotopic measurements accompanied the CVI inlet sampling at the Zeppelin Observatory  
to assist in source identification of water vapor and air mass history. Water vapor concentration and isotopic ratios of oxygen  
( $\delta^{18}\text{O}$ ) and hydrogen ( $\delta\text{D}$ ) were measured using a Picarro L2130-i isotope and gas concentration analyzer (Picarro, Inc., USA).

Deuterium excess (d-excess or d) values were computed in the form of  $d = \delta D - 8 \cdot \delta^{18}O$  (Dansgaard, 2012). The Picarro analyzer was also located in the Zeppelin Observatory (Figure 1). Inlet tubing ( $\approx 3$  m [in length](#)) sampled ambient air directly above the roof of the laboratory building [approximately 3 m a few meters](#) from the CVI. Isotopic observations began on 14 November 2019 and continued through the end of December 2020 to overlap with most of the cloud observation window.

To calibrate the water vapor isotopic measurements, the Picarro analyzer is connected to a Picarro Standards Delivery Module (SDM). Data calibration and processing for the measurements at Zeppelin Observatory follow those made at Pallas, Finland, on a similar instrument (Bailey et al., 2021). Every  $\approx 24$  hours, the SDM supplied two water samples of known isotopic composition that bracketed the range of isotopic measurements to standardize the measurements. The two standards used were USGS45 ( $\delta^{18}O = -2.238\text{‰}$ ,  $\delta D = -10.3\text{‰}$ ) and USGS49 ( $\delta^{18}O = -50.55\text{‰}$ ,  $\delta D = -394.7\text{‰}$ ). These standards were used to correct for any offsets to the VSMOW-SLAP scale and assess any instrument drift during the measurement period, which was minimal [for this period](#). Given the low water vapor concentration at times during this measurement period ( $< 1000$  ppm), it is necessary to correct any instrument bias that might exist at these lower concentrations (Steen-Larsen et al., 2013). A humidity experiment was carried out at the time of installation of the instrument and followed the protocol described by Akers et al. (2020) [that](#) included the measurement of the two standard waters over a range of water vapor concentrations regulated by dry air. A humidity response curve was developed and applied to the dataset. Additional data quality control protocols followed the methods described by Bailey et al. (2021). Once quality control and calibrations were conducted, water vapor concentration and isotopic ratios ( $\delta^{18}O$ ,  $\delta D$ , d-excess) were aggregated into 5-minute averages. The data were further aggregated to only times when the CVI was sampling to appropriately pair the isotopic observations with a given CE. Given the instrument analytical error and error in the calibration process, we estimate uncertainty to be  $< 0.3\text{‰}$  for  $\delta^{18}O$ ,  $< 1.1\text{‰}$  for  $\delta D$ , and  $< 2.1\text{‰}$  for d-excess. Error values are highest when water vapor concentration is lowest. However, for the purpose of this analysis, we only focused on times when clouds were present, which are related to times of relatively higher water vapor content, and thus the error in the isotopic measurements is generally lower than they would be across the entire dataset. Importantly, these instrument- and analysis-based errors are significantly lower than the natural variability explored in this study.

## 2.5 Cloud type classification

Unlike in situ cloud ~~residual~~-sampling at the Zeppelin Observatory, the Cloudnet dataset was retrieved for the region around the village of Ny-Ålesund approx. 2 km away from the observatory (Nomokonova et al., 2019). Using a combination of remote sensing techniques, a vertically-resolved cloud classification of the air column is obtained (Illingworth et al., 2007). This classification is explained in depth for Ny-Ålesund in Nomokonova et al. (2019, 2020). In short, at 20-meter intervals, the air column is classified according to its physical properties. This covers clear sky (CS), cloud droplets (CD), drizzle (DR), cloud droplets and drizzle (DR+CD), ice crystals (I), ice crystals and supercooled droplets (I+SCD), melting ice (MI), melting ice and cloud droplets (MI+CD), aerosol (A), insects (Ins) and aerosol and insects (A+Ins). Here, we ~~focus on an altitude analyze altitudes~~ of 400 to 600 meters [to reflect measurements taken at the Zeppelin Observatory altitude \(475 meters asl\)](#). Potential problems of this approach to cloud classification could include cases where the the cloud over Ny-Ålesund might not be the same as that at the Zeppelin mountain or where a cloud is present at one site and not at the other. However, given the long



sampling times (longer than 30 min), there is a good chance that the cloud would be present at both sites for at least a portion of the sampling time, which is sufficient for CE classification. Table S1 describes all CE and the availability of Cloudnet data.

190 For each CE, an ice-to-droplet ratio is derived using the Cloudnet data set. As previously done in Karlsson et al. (2021), this value is calculated as the ratio of ice-related classification points (I, I+SCD, MI and MI+CD) to droplet-related classification points (CD, DR and CD + DR). For those CE with a ~~mixed~~ ratio between ice and liquid classifications ( $>+10\%$  and  $<90\%$ ), a mixed-phase cloud (MPC) classification is given. The Cloudnet data ~~was also used to obtain~~ also provides the height of the cloud top ~~following the work by Chellini et al. (2022)~~ Chellini et al. (2022), but we have chosen to manually assess the lowest level cloud top height based on the column profile.

## 195 2.6 Auxiliary parameters

The ambient air temperature and relative humidity (at the Zeppelin Observatory) were measured by a weather station coupled to the CVI. Furthermore, the column air temperature was recovered from daily radio ~~sounds~~ soundings taken in the village of Ny-Ålesund (Maturilli, 2020) and using the HATPRO sensor located at the AWIPEV station (Rose et al., 2005). These air temperature curves were used to recover the ~~daily and CE~~ height in which the air temperature reached ~~values lower than~~  $-15^{\circ}\text{C}$ , in a daily (radio soundings) and per CE (HATPRO) resolution.

200 For one CE in ~~August~~ September 2020, a ~~sample with coarse mode aerosol~~ coarse-mode aerosol sample grid used for transmission electronic microscopy (TEM, for particles above  $0.7\ \mu\text{m}$  in aerodynamic diameter) ~~was successfully sampled~~ successfully sampled cloud residuals for 30 min at ~~1~~  $1\ \text{m}\ \text{min}^{-1}$  downstream of the CVI inlet and the particles were classified using the elemental composition described by Adachi et al. (2022). ~~On the TEM grid, three PBAP were successfully identified (among the 133 particles analyzed and representing around  $\approx 2\%$  of the particles collected) based on their shape and composition, confirming the presence of PBAP in the cloud residuals.~~

## 205 2.7 Back trajectory analysis

Back trajectory ensembles were initialized at a height of 250 m at the latitude and longitude of the observatory, every hour for the days in which there were valid observations. The ensemble was generated by shifting the meteorological fields, whilst keeping the initialized starting point the same; in total 27 back trajectories were initialized in each ensemble. The length of the back trajectories was restricted to 5 days. Data points along each and every back trajectory (i.e. endpoints) were selected only if they resided within the mixed layer (as defined by the model/HYSPLIT output). Previous work by Karlsson et al. (2021) showed that increasing or decreasing the mixing layer height does not significantly affect the general contribution of surface types. The endpoints were temporally and spatially collocated with gridded sea ice daily data derived from satellite observations (Copernicus Climate Change Service (C3S) Climate Data Store (CDS), accessed on 12/07/2023) to ascertain the surface type directly below each endpoint, within the mixed-layer. All back trajectories were carried out using the Hybrid Single-Particle Lagrangian Integrated Trajectory model (HYSPLIT V5.2.1, Draxler et al., 1998; Stein et al., 2015), with the Global Data Assimilation System (GDAS)  $1^{\circ}\times 1^{\circ}$  archive data being used for the metrological fields (<https://www.ready.noaa.gov/data/archives/gdas1/>, last access: 12/07/2023). The Python package PySPLIT (Cross, 2015) was used to generate the ensemble back trajectories.

During the period from June 2019 to December 2020, the CVI sampled ~~We collected~~ 209 CE that lasted of at least 30 minutes ~~duration from June 2019 to December 2020~~. For each CE, the coarse-mode ~~aerosol~~ cloud residuals (optical diameter  $>0.8 \mu\text{m}$ ) ~~was-were~~ characterized in a single-particle manner by the MBS, resolving the fPBAP contribution for each CE.

225 First, we present an overview ~~and a detailed characterization~~ of fPBAP found in cloud residuals (Section ~~3.1 and 3.23.1~~ and 3.2). Second, ~~we include an analysis of the annual cycle of all characterized CE (Sect. 3.3) and their source allocation (Sect. 3.4). Finally, we present~~ a case study of a mixed-phase cloud event ~~with the highest concentration of fPBAP (MPC, Sect. 3.5), 3.5). Similar case studies for~~ a liquid phase ~~cloud event (Sect. ??) and an ice cloud event (Sect. ??) will be phase~~ cloud are briefly presented and discussed ~~The last part includes an analysis of the annual cycle of all characterized CE (Sect. 3.3) and their source allocation (Sect. 3.4) in sections 1.1 and 1.2 of the SI.~~

### 230 3.1 Characterization of fluorescent primary biological particles within cloud residuals

A summary of fPBAP found in cloud residuals throughout the campaign is shown in Table 1. Over 209 CE, representing a total of 812 hours ~~In total~~, 527 fPBAP were detected by the MBS within cloud residuals ~~This accounts (Table 1), accounting~~ for less than 1 particle per cloud hour ~~(or 18.9 liters sampled by the MBS). However, extremely low fPBAP concentrations are in the range of typical high-temperature INP concentrations found in the Arctic ( $10^{-4}$ – $10^{-1}$ , at activation temperature  $\approx -15^\circ\text{C}$ , Creamean et al. (2022); Sze et al. (2023)).~~ In summer, fPBAP ~~cloud residual~~ concentrations ranged from  $10^{-3}$ – $10^{-2} \text{L}^{-1}$  (mean:  $8.1 \cdot 10^{-3} \text{L}^{-1}$ ) ~~and contributed contributing~~ up to 5% (mean: 0.03%) of the ~~coarse mode coarse-mode cloud residual~~ particles. In winter, both the concentration and the relative contribution ~~to the coarse aerosol particles~~ were lower (mean:  $4.2 \cdot 10^{-3} \text{L}^{-1}$  and 0.005%, respectively). ~~These fPBAP concentrations are in the range of typical high-temperature INP concentrations found in the Arctic ( $10^{-4}$ – $10^{-1} \text{L}^{-1}$ , at activation temperature  $\approx -15^\circ\text{C}$ , Creamean et al. (2022); Sze et al. (2023); Pereira F~~  
 240 ~~).~~ Of all sampled CE in summer and winter, 67% and 45% contained at least one ~~cloud residual fPBAP~~ fPBAP cloud residual, respectively. ~~Moreover, despite Despite~~ PBAP contributing significantly to the INP population in the Arctic (e.g., Pereira Freitas et al., 2023) they are not the only source (e.g., Tobo et al., 2019). ~~Given Nonetheless, given~~ the relatively high number of clouds containing fPBAP and the susceptibility of Arctic clouds to have their phase modulated by low concentrations of INP (Prenni et al., 2007), fPBAP could be relevant ~~to in~~ aiding cloud glaciation processes in Arctic low-level clouds.

### 245 3.2 Transmission electron microscopy of coarse cloud residuals

For a CE on the 22nd of ~~August September~~ 2020, one TEM grid with identified PBAP was successfully sampled for 30 minutes ~~behind downstream of~~ the CVI which overlapped with the MBS sampling. Using the elemental analysis described by Adachi et al. (2020, 2022), we assessed the probable nature of the aerosol in the ~~coarse mode coarse-mode~~ sampled on the grid. The TEM images (Figure 2-A,B,C) show 3 PBAP that were part of cloud residuals (out of the 133 particles analyzed from the TEM  
 250 grid or around 2%). During the same ~~cloud event CE~~ CE, the MBS measured 5 fPBAP cloud residuals (Figure 2-D), accounting for 0.05% of the total ~~coarse mode coarse-mode~~ particles. Webcam images of the cloud are also shown in Figure 2-D. It should be



noted that the cut sizes for the TEM grid and the MBS slightly differ ( $0.7 \mu\text{m}$  in aerodynamic and  $0.8 \mu\text{m}$  in optical diameter, respectively). The ~~deuterium-excess d-excess~~ for this CE was  $0.3\%$ , which is a very low number, signaling that this cloud (~~water vapor~~) ~~was probably locally~~'s ~~water vapor was probably regionally~~ sourced. Unfortunately, Cloudnet data was not available  
255 for this CE, so no assessment of the cloud phase could be made.

To the best of our knowledge, this is the first time PBAP were directly imaged in cloud residuals (as opposed to being collected in a cloud water sample, Bauer et al., 2002), directly indicating their possible role as cloud condensation nuclei and/or INP. However, it is difficult to draw further conclusions based on one sample, thus this result should be taken as a supporting analysis to the more comprehensive MBS analysis.

### 260 3.3 Case I: Mixed-phase cloud

~~For the second week of September, the Zeppelin Observatory was continuously in cloud from the 5th to the 8th of September 2020. At the beginning, the Cloudnet classification was mostly consistent with a liquid cloud, with an increase in ice contribution towards the second half. For the first CE the ice fraction was 12%. The cloud glaciated and transitioned to containing almost only ice crystals before dissipating (up to 97% of ice, Figure 5-A). Visibility remained below 1000 meters for most of the  
265 cloud. Wind speeds hovered around 2 m/s with a persistent southerly direction except for a few hours when it switched to northerly winds (Figure 5-B). These long-lasting MPC are common for the Arctic (Morrison et al., 2012).~~

~~The d-excess from the cloud water vapor started at  $-5\%$  and ended at around  $0\%$ . This small change and the overall low values signal that the air mass was of local origin (Kopeck et al., 2016), indicating that the cloud water vapor was regionally sourced (Figure 5-C). However, it should be kept in mind that the aerosol and water vapour source might not be identical.  
270 The aerosol population could for example be a mix between regional (e.g., Pereira Freitas et al., 2023) and transported sources (e.g., Behrenfeldt et al., 2008; Geng et al., 2010). The coarse-mode aerosol comprises of larger particles that are effectively removed by dry and wet deposition (Stopelli et al., 2015), but can sometimes be transported to the Arctic from lower latitudes (Behrenfeldt et al., 2008). The precipitation process along the path of transported air masses will lead to the depletion of d-excess and the wet removal of aerosol. Although we cannot use the d-excess to decisively link the cloud aerosol population to  
275 regional sources, the d-excess values and additionally performed trajectory calculations (Figure S2) point to a more pronounced contribution of regional sources of both vapor and aerosol.~~

~~The cloud temperature at 475 m above sea level was  $7.5^\circ\text{C}$  at the start of the cloud and continuously dropped to  $0^\circ\text{C}$  towards the end of the cloud as it glaciated. For this day, the air temperature reached values of  $-15^\circ\text{C}$  only at approximately 4000 meters above sea level and the height of the cloud top at approximately 1600 meters (temperature at cloud top height:  $\approx -8^\circ\text{C}$ , Figure  
280 S3). Thus, a likely explanation for the presence of ice within this cloud is ice nucleation being started by high-temperature INP (Fan et al., 2017), of which fPBAP are part of (Tobo et al., 2013), or secondary ice formation due to, e.g. ice crystals being deposited by clouds higher up in the atmosphere (Lohmann et al., 2016).~~

~~As the cloud developed, fPBAP were clearly detected by the MBS within the cloud residuals. A total of 58 fPBAP were found within the cloud (over 4 CE) accounting for 2 in every  $10^4$  coarse mode particles. The presence of fPBAP could be  
285 one of the explanations for cloud glaciation at temperatures at which the presence of high temperature INP would be required.~~

However, further studies assessing the role of other glaciation mechanisms are required to fully establish the impact of fPBAP (and INP) on low-level Arctic clouds. Nevertheless, a study by Carlsen and David (2022) suggests that MPC in the Arctic and Antarctic would only be feasible year-round, should such high-temperature INP be present.

### 3.3 Case II: Liquid cloud

290 This is a case study that includes five CE that took place between 12 and 17 July 2020. The Cloudnet classification of these CE generally remained between CD and DR (Figure ??-A), similar to that of a liquid cloud. Here, some of the CE, when visibility was low, did not completely coincide with the expected Cloudnet classification (e.g. Cloudnet classified the air above Ny-Ålesund as aerosol/clear sky, while the low visibility clearly indicated a presence of clouds at the observatory), exemplifying the differences between what was measured at the peak of the Zeppelin mountain and that above the Ny-Ålesund  
295 village. This discrepancy is due to the differences in wind pattern between the two sites (Pasquier et al., 2022). This was one limitation of this study, as sophisticated cloud probes were not available at such a comprehensive time frame as the methods used here.

The cloud persisted over northerly winds and low to medium wind speeds (Figure ??-B). Deuterium excess values were quite low (0–5‰) and followed quite close the ambient air temperature that stayed always above 2.5 °C (Figure ??-C). During  
300 all 5 CE, the altitude at which the temperature reached –15 °C hovered around 4800 meters and cloud top height was highly variable between 4 and 8 km (Figure S4). In fact, ice was present in the cloud at an altitude of 2000 meters. Given the high temperatures within the cloud at the Zeppelin Observatory, not even the presence of high-temperature INP would give rise to ice formation within it. An indication that despite the presence of INP, meteorological conditions were not favorable for ice formation at the lower levels of the cloud, but ice formation was seen higher in the column at temperatures still above –15 °C.  
305 However, it is not possible to clearly separate whether it is the result of primary ice nucleation or other glaciation mechanisms above that initiate secondary ice formation below.

Several fPBAP were sampled by the MBS during these CE (Figure ??-D). Removing the 4th CE of this case study, in which the MBS was not fully operational, the MBS sampled 99 fPBAP, representing approximately 0.01% (or 1 in every 10<sup>4</sup> particles) of the total coarse mode. Throughout the summer, fPBAP are ubiquitous at the Zeppelin Observatory (Pereira Freitas et al., 2023)  
310 and the results presented here show directly that they are present within cloud residuals and possibly acted as cloud condensation nuclei. Under suitable conditions, they could contribute to glaciation and MPC formation.

### 3.3 Case III: Ice cloud

This is a case study of 3 consecutive CE that took place during October 28th and 29th, 2020. These CE all had completely glaciated clouds (Figure ??-A). Across these events, significant cooling occurred (from –2.5 to –10 °C) as the winds shifted  
315 to coming from the north and strengthened (10 ms<sup>-1</sup>). Along with these changes, the d-excess shifted from relatively low values (0–5‰) to relatively high values (15–20‰), signaling a more transported source. During this cloud, the MBS detected 10 fPBAP (0.015% contribution to the coarse mode, Figure ??-D). The increase in deuterium excess during these events points to a shift to a more distant source of moisture in this winter case, and the temperature is low enough so that ice nucleation

could have been started by INP of different activation temperatures along the cloud column. However, as mentioned above, the moisture and aerosol sources can, but not necessarily, be the same; thus, the deuterium excess values are only indicative. Given the meteorological conditions (Figure S5), little can be said about the influence of PBAP on this cloud. However, this shows that fPBAP are as evenly present in clouds as they are in the atmosphere throughout the year.

### 3.3 Annual cycle of cloud parameters

For all 209 CE measured during the years 2019 and 2020, several parameters were averaged for each CE, such as of the 209 CE, including ambient temperature, deuterium excess d-excess and ice-to-droplet ratio; these were then which were subsequently grouped by month (Figure 3). Above panel A of Figure 3 the number of CE (# cloud events) is shown along with the total hours sampled (# hours sampled) for each month of the year. As can be seen, most CE were concentrated in summer, when sampling conditions were generally better and it is known. It is also documented that low-level clouds are also more present in the summer-late summer (early fall) months (Illingworth et al., 2007; Taylor et al., 2019; Curry and Ebert, 1992; Maturilli and Ebell, 2018).

The concentration of coarse-mode coarse-mode aerosol particles within CE was generally lower in summer and higher in winter months (Figure 3-A), due to the increased contribution of sea spray in the fall and winter months (Adachi et al., 2022; Zieger et al., 2020). This seasonality is due to increased wind speeds and prevalence of storms in winter, that generate nascent sea spray from ocean surfaces and lift sea salt rich snow from ice covered ocean (Adachi et al., 2022). The opposite behavior is observed by the contribution of fPBAP to the coarse-mode coarse-mode (Figure 3-A), which was much higher in summer than in winter. The annual cycle of the cloud fPBAP population reflects that of the general fPBAP population at the Zeppelin Observatory (Pereira Freitas et al., 2023). These seem to reflect results seem to confirm the expectation that fPBAP would act as efficient cloud nuclei (Ariya et al., 2009). At the beginning and end of summer, when the contribution of fPBAP is higher and meteorological conditions are favorable, they potentially could also contribute to the formation of MPC by acting as INP.

The deuterium excess d-excess within the CE (Figure 3-B) shows high values for winter, while showing and low values for the remainder of the year. This implies that the moisture in winter air masses was mainly sourced from long-range transport (Kopec et al., 2016). This agrees well with reports on the influence of lower latitudes on the Arctic aerosol population in winter (Sharma et al., 2006). For the lower d-excess for the remainder of the year, a low d-excess implies that moisture, and possibly PBAP, were more regionally and/or locally sourced (Kopec et al., 2016; Delattre et al., 2015; Froehlich et al., 2002). These results point to a possible locally driven regulation of cloud formation around Svalbard, to a degree which we cannot estimate. The d-excess observations are further confirmed by combined with back trajectory analyses linking link lower values to long-range transport from terrestrial sources (Figure S2)- S6). These results point to a more pronounced terrestrial origin of cloud residual fPBAP, corroborating previous work where fPBAP detected at Zeppelin Observatory were found to originate from regional and land-based sources (Pereira Freitas et al., 2023), including the polar semideserts that dominate the tundra of Svalbard (Welker et al., 1993; Wookey et al., 1995). Nonetheless, the ocean and sea ice can still be a significant source of fPBAP and INP, especially in winter (Creamean et al., 2019; Pereira Freitas et al., 2023). Moreover, the Svalbard region is

notorious for being strongly affected by the Arctic amplification, prompting a dramatic change in annual sea-ice coverage (Urbański and Litwicka, 2022). Thus, although our results point to terrestrial sources, fPBAP sourced from regional marine and ice sources can still significantly contribute to the fPBAP population to a degree that is hard to estimate using our methods. DNA based techniques, such as those applied by Šantl-Temkiv et al. (2019) could better constrain the sources of fPBAP in the Arctic.

The ice-to-droplet ratio (Figures 3-C) shows that low-level clouds at Ny-Ålesund during the colder months (1-5 and 9-12 January-April and September-December) are mainly represented by ice clouds, and clouds during the month of July whereas for July they are mainly represented by liquid droplets. For June and August, most of the clouds included both phases and as such were most likely clouds were MPC, which reflects the findings of Mioche et al. (2015). Figure 3-C shows that MPC were mostly present between 400 and 600 meters at Ny-Ålesund at the beginning and end of summer, when there are suitable meteorological conditions and a higher contribution of PBAP-fPBAP to coarse-mode aerosol.

The ambient temperature at 475 meters above sea level asl reached values as low as  $-25^{\circ}\text{C}$  in winter and values as high as  $10^{\circ}\text{C}$  in summer (Figure 3-D). In the months that transition from summer to winter, such as May-June and August-September, the air temperature was on average around  $0^{\circ}\text{C}$ . For the months of May through September, the altitude in which ambient temperature reached  $-15^{\circ}\text{C}$  sat above only at altitudes higher than 2500 meters, as. This can be seen in Figure 3-E), derived by both daily radio soundings and continuous HATPRO vertical temperature profiling above the village of Ny-Ålesund for each individual CE. The cloud top height of low-level clouds was much higher in the beginning of the year, reaching its minima in summer, where it stayed below 2500 meters. Thus, the temperatures across the cloud-air columns in summer point to facilitated ice formation in the presence the requirement of high-temperature INP for ice formation to occur.

These results are an early but clear indication of the contribution of fPBAP to MPC in the Arctic. In the future, For a more comprehensive study that uses understanding of the PBAP's role in Arctic MPC formation, a combination of single-particle cloud particle probes (which also allows the differentiation probes and CVI would allow for distinction between individual ice and droplet particles) at the Zeppelin observatory collocated with the CVI measurements and a detailed assessment of the cloud column is warranted to fully comprehend the degree in which fPBAP are acting as INP and thus play a role in Arctic MPC formation.

### 3.4 Potential sources of fluorescent primary biological aerosol particles within Relationship between cloud residuals phase, bioaerosol contribution and isotope ratio

A comparison of all clouds that had concurrent deuterium excess and Cloudnet data available is shown in Figure 4 by showing the deuterium excess Figure 4 shows the d-excess rate vs. the fPBAP contribution to the coarse mode coarse mode cloud residual concentration for the three different cloud regimes (as defined by the ice-to-droplet ratio) separately for the three cloud regimes grouped by winter and summer seasons. In Figure 4-A, liquid clouds appear only in summer and present high ambient air temperatures, as expected (Ebell et al., 2020). Low d-excess values link the water vapor or moisture to air masses of predominantly local origin; these clouds also show a reasonable contribution of fPBAP. As previously noted by Gierens et al. (2020), local-scale aerosol sources could be important for cloud formation and evolution in the Arctic.

regional origin. These clouds had a fPBAP contribution of 0.01%. MPC are present mainly in summer and at mild temperature (from  $-5^{\circ}\text{C}$  to  $5^{\circ}\text{C}$ , as shown in Figure 4-B). Most of them have a reasonable contribution of fPBAP to the coarse mode and originate from local air masses, as indicated by the low d-excess values. These results agree with those of Gierens et al. (2020), where they estimate an increased contribution of local sources in summer.

Ice clouds are For MPC at mild temperatures (from  $-5^{\circ}\text{C}$  to  $5^{\circ}\text{C}$ ), fPBAP contribution was 0.01% or higher. Ice clouds were predominantly seen in winter, but some are seen in summer (Figure 4-C). Those in summer are observed in summer were present at mild temperatures ( $-5^{\circ}\text{C}$  to  $5^{\circ}\text{C}$ ) and typically had a low d-excess. Some of the summer value. A few ice clouds were highly enriched in fPBAP (values above 0.025%) with d-excess rates at around 10%, indicating that some ice clouds could have formed through the presence of INP, of which fPBAP are a significant part. Furthermore, these clouds are strongly related to regional and/or local sources of air mass and aerosols, which were previously reported to be the main contributors to fPBAP in the Arctic (Pereira Freitas et al., 2023) a mix between regional and transported sources.

These results show that summer clouds containing ice were present at mild temperatures, often containing fPBAP ( $>0.01\%$ ), indicating the role of fPBAP in ice formation. For all cloud phase regimes, fPBAP were mostly present at lower d-excess values. Regional aerosol sources are important for cloud formation and evolution in the Arctic (Gierens et al., 2020), and this seems to be reflected here.

### 3.5 Mixed-phase cloud events analysis

From the 5th to the 8th of September 2020, the Zeppelin Observatory was continuously in cloud. Initially, the Cloudnet classification was mostly consistent with a liquid cloud, with an increase in ice contribution towards the second half. For the first CE the ice fraction was 12%. The cloud glaciated and transitioned to containing almost only ice crystals before dissipating or migrating (up to 97% of ice, Figure 5-A). Visibility remained below 1000 meters for most of the cloud. Wind speeds hovered around  $2\text{ m s}^{-1}$  with a persistent southerly direction except for a few hours when it switched to northerly winds (Figure 5-B). These long-lasting MPC are common for the Arctic (Morrison et al., 2012).

The d-excess from the cloud water vapor started at  $-5\%$  and ended at around  $0\%$ . This small change and the overall low values signal that the air mass was of regional origin (Kopeck et al., 2016), (Figure 5-C). The water vapor and aerosol source might not be identical, whereas the latter could be a mix between regional (e.g., Pereira Freitas et al., 2023) and long-range transported emissions (e.g., Behrenfeldt et al., 2008; Geng et al., 2010; Creamean et al., 2022). Coarse-mode aerosol comprises of larger particles that are effectively removed by dry and wet deposition (Stopelli et al., 2015), but are occasionally transported to the Arctic from lower latitudes (Behrenfeldt et al., 2008). The precipitation process along the path of transported air masses will lead to the depletion of d-excess values and the wet removal of coarse-mode aerosol. However, we cannot use the d-excess to decisively link the cloud aerosol population to regional sources.

The cloud temperature at 475 m above sea-level was  $7.5^{\circ}\text{C}$  at the start of the cloud and continuously dropped to  $0^{\circ}\text{C}$  towards the end of the cloud as it glaciated. For this day, the air temperature reached values of  $-15^{\circ}\text{C}$  only at approximately 4000 meters asl and the height of the cloud top was approximately 1600 meters (temperature at cloud top height:  $\approx -8^{\circ}\text{C}$ , Figure S7). Thus, a likely explanation for the presence of ice within this cloud is ice nucleation being started by high-temperature INP

(Fan et al., 2017), of which fPBAP are part of (Tobo et al., 2013), or secondary ice formation due to, e.g. ice crystals being deposited by clouds higher up in the atmosphere (Lohmann et al., 2016).

425 As the cloud developed, fPBAP were clearly detected by the MBS within the cloud residuals. A total of 58 fPBAP were found within the cloud (over 4 CE) accounting for 2 in every  $10^4$  coarse-mode particles. The presence of fPBAP could be one of the explanations for cloud glaciation at temperatures at which the presence of high-temperature INP would be required. However, further studies assessing the role of other glaciation mechanisms (such as precipitation from clouds higher in the column) are required to fully establish the impact of fPBAP (and INP) on low-level Arctic clouds.

## 4 Conclusions

430 ~~In this study, we used single particle fluorescence spectroscopy to identify fluorescent primary bioaerosol. Within this work, we showed that fluorescent primary biological aerosol particles (fPBAP) are found within cloud residuals and possibly contributed to the formation of low-level Arctic clouds. These cloud residuals were collected. This was achieved, for the first time, by direct observations using a ground-based counterflow virtual impactor inlet installed at the Zeppelin Observatory near Ny-Ålesund, Svalbard, over the span of a year and a half. fPBAP cloud residuals combined with online and offline particle sampling techniques. This approach avoided indirect proof of the relevance of fPBAP on cloud properties, for example, when using correlations of INP with fPBAP concentrations as done previously (Pereira Freitas et al., 2023). fPBAP exhibited higher concentrations ( $10^{-3}$ – $10^{-2}$  L $^{-1}$ ) and a greater contribution contributions (0.1 to 1 in  $10^3$  particles) to the coarse-mode aerosol during the cloud residuals in summer compared to winter ( $10^{-4}$ – $10^{-3}$  L $^{-1}$ , and 1 in  $10^4$ – $10^5$  particles, respectively). Water. In summer, water vapor isotope data linked these fPBAP cloud residuals clouds to regional sources. Despite their low abundance, the presence of fPBAP in the cloud residuals was confirmed by transmission electronic microscopy. Our analysis of meteorological data and cloud classification data using remote sensing, showed that the~~ Thus, fPBAP most likely originated from the biosphere around Svalbard. The presence of fPBAP was associated with the prevalence of mixed phase clouds (MPC) at the beginning and end of summer. ~~This suggests that MPC formation would be possible if high-temperature INP were present. Therefore~~ Here, we present experimental and direct evidences that fPBAP, possibly from the local biosphere, could contribute to cloud formation in the Arctic. fPBAP contribute to ice formation in Arctic low-level clouds. However, cloud formation is a complex phenomena involving meteorology as well as interlinked cloud and aerosol microphysical and chemical processes. Thus, the degree to which they fPBAP influence cloud glaciation and MPC formation in general would require further investigation both experimental (e.g. better by quantitative assessment of the cloud phase using single particle cloud probes) but also using modelling approaches. Future work should also include filter sampling for genetic analysis to identify the biological material and origin, in addition to parallel sampling of bioaerosols within cloud residuals and interstitial aerosol to assess whether certain microorganisms are more likely to act as cloud condensation nuclei.

445

450



*Data availability.* The data is available at the Bolin Centre for Climate Research database (DOI:10.17043/zeppelin-freitas-2023-bioclouds-1).

*Author contributions.* GF, RK and PZ performed MBS and GCVI measurements. KA performed TEM measurements. GF analyzed MBS, GCVI and auxiliary data and wrote manuscript with contributions from all co-authors. BK, AH and JW performed water isotope measurements and performed analysis. DH-R performed back trajectory analysis. KEY provided valuable insights to the discussion and writing of the manuscript. PZ conceived the study. All authors read and commented on the final version of the manuscript.

*Competing interests.* At least one of the (co-)authors is a member of the editorial board of Atmospheric Chemistry and Physics.

*Acknowledgements.* The authors would like to acknowledge the Norwegian Polar Institute for their long-term support at Zeppelin Observations. This research was supported by the Swedish Research Council (grant no. 2018-05045), the Knut och Alice Wallenbergs Stiftelse (ACAS project grant no. 2016.0024) and the the Swedish Environmental Agency (Naturvårdsverket). This project has received funding from the European Union's Horizon 2020 research and innovation programme under Grant Agreement 821205 (FORCeS). This project has received funding from the European Union's Horizon 2020 research and innovation programme under grant agreement no. 101003826 via project CRiceS (Climate Relevant interactions and feedbacks: the key role of sea ice and Snow in the polar and global climate system). We thank the Environmental Research and Technology Development Fund (JPMEERF20232001) of the Environmental Restoration and Conservation Agency of Japan and the Arctic Challenge for Sustainability II (ArCS II) (JPMXD1420318865). Water isotopic measurements at Zeppelin were supported by the Academy of Finland award to Welker and Hubbard. The authors thank Valtteri Hyöky for on-site support and data processing for the isotopic measurements at Zeppelin. The authors recognize NPI for its long-term support of measurements at the Zeppelin Observatory.

## References

- 470 Adachi, K., Oshima, N., Gong, Z., De Sá, S., Bateman, A. P., Martin, S. T., De Brito, J. F., Artaxo, P., Cirino, G. G., Iii, A. J., and Buseck, P. R.:  
Mixing states of Amazon basin aerosol particles transported over long distances using transmission electron microscopy, *Atmospheric  
Chemistry and Physics*, 20, 11 923–11 939, <https://doi.org/10.5194/acp-20-11923-2020>, 2020.
- Adachi, K., Tobo, Y., Koike, M., Freitas, G., Zieger, P., and Krejci, R.: Composition and mixing state of Arctic aerosol and cloud residual  
particles from long-term single-particle observations at Zeppelin Observatory, Svalbard, *Atmospheric Chemistry and Physics*, 22, 14 421–  
475 14 439, <https://doi.org/10.5194/acp-22-14421-2022>, 2022.
- Akers, P. D., Kopec, B. G., Mattingly, K. S., Klein, E. S., Causey, D., and Welker, J. M.: Baffin Bay sea ice extent and synoptic moisture  
transport drive water vapor isotope ( $\delta^{18}\text{O}$ ,  $\delta^2\text{H}$ , and deuterium excess) variability in coastal northwest Greenland, *Atmospheric Chemistry  
and Physics*, 20, 13 929–13 955, <https://doi.org/10.5194/acp-20-13929-2020>, 2020.
- Ariya, P. A., Sun, J., Eltouny, N. A., Hudson, E. D., Hayes, C. T., and Kos, G.: Physical and chemical characterization of bioaerosols - Im-  
480 plications for nucleation processes, *International Reviews in Physical Chemistry*, 28, 1–32, <https://doi.org/10.1080/01442350802597438>,  
2009.
- Bailey, H., Hubbard, A., Klein, E. S., Mustonen, K. R., Akers, P. D., Marttila, H., and Welker, J. M.: Arctic sea-ice loss fuels extreme  
European snowfall, *Nature Geoscience*, 14, 283–288, <https://doi.org/10.1038/s41561-021-00719-y>, 2021.
- Bauer, H., Kasper-Giebl, A., Löflund, M., Giebl, H., Hitzenberger, R., Zibuschka, F., and Puxbaum, H.: The contribution of bacteria and  
485 fungal spores to the organic carbon content of cloud water, precipitation and aerosols, Tech. rep., [www.elsevier.com/locate/atmos](http://www.elsevier.com/locate/atmos), 2002.
- Bauer, H., Giebl, H., Hitzenberger, R., Kasper-Giebl, A., Reischl, G., Zibuschka, F., and Puxbaum, H.: Airborne bacteria as cloud condensa-  
tion nuclei, *Journal of Geophysical Research: Atmospheres*, 108, <https://doi.org/10.1029/2003jd003545>, 2003.
- Behrenfeldt, U., Krejci, R., Ström, J., and Stohl, A.: Chemical properties of Arctic aerosol particles collected at the Zeppelin sta-  
tion during the aerosol transition period in May and June of 2004, *Tellus B: Chemical and Physical Meteorology*, 60, 405–415,  
490 <https://doi.org/10.1111/j.1600-0889.2008.00349.x>, 2008.
- Bonne, J., Steen-Larsen, H. C., Risi, C., Werner, M., Sodemann, H., Lacour, J., Fettweis, X., Cesana, G., Delmotte, M., Cattani, O., Valle-  
longa, P., Kjær, H. A., Clerbaux, C., Sveinbjörnsdóttir, E., and Masson-Delmotte, V.: The summer 2012 Greenland heat wave: In situ and  
remote sensing observations of water vapor isotopic composition during an atmospheric river event, *Journal of Geophysical Research:  
Atmospheres*, 120, 2970–2989, <https://doi.org/10.1002/2014JD022602>, 2015.
- 495 Bonne, J.-L., Behrens, M., Meyer, H., Kipfstuhl, S., Rabe, B., Schönicke, L., Steen-Larsen, H. C., and Werner, M.: Resolving the controls of  
water vapour isotopes in the Atlantic sector, *Nature Communications*, 10, 1632, <https://doi.org/10.1038/s41467-019-09242-6>, 2019.
- Carlsen, T. and David, R. O.: Spaceborne Evidence That Ice-Nucleating Particles Influence High-Latitude Cloud Phase, *Geophysical Re-  
search Letters*, 49, 1–11, <https://doi.org/10.1029/2022GL098041>, 2022.
- Chellini, G., Gierens, R., and Kneifel, S.: Ice Aggregation in Low-Level Mixed-Phase Clouds at a High Arctic Site: Enhanced  
500 by Dendritic Growth and Absent Close to the Melting Level, *Journal of Geophysical Research: Atmospheres*, 127, 1–23,  
<https://doi.org/10.1029/2022JD036860>, 2022.
- Copernicus Climate Change Service (C3S) Climate Data Store (CDS): Copernicus Climate Change Service (C3S) (2020): Sea ice concen-  
tration daily gridded data from 1979 to present derived from satellite observations, <https://doi.org/10.24381/cds.3cd8b812>.

- Crawford, I., Gallagher, M. W., Bower, K. N., Choulaton, T. W., Flynn, M. J., Ruske, S., Listowski, C., Brough, N., Lachlan-Cope, T.,  
505 Fleming, Z. L., Foot, V. E., and Stanley, W. R.: Real-time detection of airborne fluorescent bioparticles in Antarctica, *Atmospheric Chemistry and Physics*, 17, 14 291–14 307, <https://doi.org/10.5194/acp-17-14291-2017>, 2017.
- Crawford, I., Topping, D., Gallagher, M., Forde, E., Lloyd, J. R., Foot, V., Stopford, C., and Kaye, P.: Detection of airborne biological particles in indoor air using a real-time advanced morphological parameter uv-lif spectrometer and gradient boosting ensemble decision tree classifiers, *Atmosphere*, 11, <https://doi.org/10.3390/atmos11101039>, 2020.
- 510 Creamean, J. M., Kirpes, R. M., Pratt, K. A., Spada, N. J., Maahn, M., De Boer, G., Schnell, R. C., and China, S.: Marine and terrestrial influences on ice nucleating particles during continuous springtime measurements in an Arctic oilfield location, *Atmospheric Chemistry and Physics*, 18, 18 023–18 042, <https://doi.org/10.5194/acp-18-18023-2018>, 2018.
- Creamean, J. M., Cross, J. N., Pickart, R., McRaven, L., Lin, P., Pacini, A., Hanlon, R., Schmale, D. G., Cenicerros, J., AydeU, T., Colombi, N., Bolger, E., and DeMott, P. J.: Ice Nucleating Particles Carried From Below a Phytoplankton Bloom to the Arctic Atmosphere, *Geophysical Research Letters*, 46, 8572–8581, <https://doi.org/10.1029/2019GL083039>, 2019.
- 515 Creamean, J. M., Barry, K., Hill, T. C., Hume, C., DeMott, P. J., Shupe, M. D., Dahlke, S., Willmes, S., Schmale, J., Beck, I., Hoppe, C. J., Fong, A., Chamberlain, E., Bowman, J., Scharien, R., and Persson, O.: Annual cycle observations of aerosols capable of ice formation in central Arctic clouds, *Nature Communications*, 13, 1–12, <https://doi.org/10.1038/s41467-022-31182-x>, 2022.
- Cross, M.: PySPLIT: a Package for the Generation, Analysis, and Visualization of HYSPLIT Air Parcel Trajectories, pp. 133–137,  
520 <https://doi.org/10.25080/Majora-7b98e3ed-014>, 2015.
- Curry, J. A. and Ebert, E. E.: Annual Cycle of Radiation Fluxes over the Arctic Ocean: Sensitivity to Cloud Optical Properties, *Journal of Climate*, 5, 1267–1280, [https://doi.org/https://doi.org/10.1175/1520-0442\(1992\)005<1267:ACORFO>2.0.CO;2](https://doi.org/https://doi.org/10.1175/1520-0442(1992)005<1267:ACORFO>2.0.CO;2), 1992.
- Dansgaard, W.: Stable isotopes in precipitation, *Tellus A: Dynamic Meteorology and Oceanography*, 16, 436, <https://doi.org/10.3402/tellusa.v16i4.8993>, 2012.
- 525 Delattre, H., Vallet-Coulomb, C., and Sonzogni, C.: Deuterium excess in the atmospheric water vapour of a Mediterranean coastal wetland: Regional vs. local signatures, *Atmospheric Chemistry and Physics*, 15, 10 167–10 181, <https://doi.org/10.5194/acp-15-10167-2015>, 2015.
- Despré, V. R., Alex Huffman, J., Burrows, S. M., Hoose, C., Safatov, A. S., Buryak, G., Fröhlich-Nowoisky, J., Elbert, W., Andreae, M. O., Pöschl, U., and Jaenicke, R.: Primary biological aerosol particles in the atmosphere: A review, *Tellus, Series B: Chemical and Physical Meteorology*, 64, <https://doi.org/10.3402/tellusb.v64i0.15598>, 2012.
- 530 Draxler, R. R., Spring, S., Maryland, U. S. A., and Hess, G. D.: An Overview of the HYSPLIT\_4 Modelling System for Trajectories, Dispersion, and Deposition, Tech. rep., 1998.
- Ebell, K., Nomokonova, T., Maturilli, M., and Ritter, C.: Radiative effect of clouds at ny-Ålesund, svalbard, as inferred from ground-based remote sensing observations, *Journal of Applied Meteorology and Climatology*, 59, 3–22, <https://doi.org/10.1175/JAMC-D-19-0080.1>, 2020.
- 535 Fan, J., Ruby Leung, L., Rosenfeld, D., and Demott, P. J.: Effects of cloud condensation nuclei and ice nucleating particles on precipitation processes and supercooled liquid in mixed-phase orographic clouds, *Atmospheric Chemistry and Physics*, 17, 1017–1035, <https://doi.org/10.5194/acp-17-1017-2017>, 2017.
- Freitas, G. P., Stolle, C., Kaye, P. H., Stanley, W., Herlemann, D. P., Salter, M. E., and Zieger, P.: Emission of primary bioaerosol particles from Baltic seawater, *Environmental Science: Atmospheres*, pp. 1170–1182, <https://doi.org/10.1039/d2ea00047d>, 2022.

- 540 Froehlich, K., Gibson, J. J., and Aggarwal, P. K.: Deuterium excess in precipitation and its climatological significance, Tech. rep., International Atomic Energy Agency (IAEA), [http://inis.iaea.org/search/search.aspx?orig\\_q=RN:34017972http://www-pub.iaea.org/MTCD/publications/PDF/CSP-13-P\\_web.pdf](http://inis.iaea.org/search/search.aspx?orig_q=RN:34017972http://www-pub.iaea.org/MTCD/publications/PDF/CSP-13-P_web.pdf), 2002.
- Fröhlich-Nowoisky, J., Kampf, C. J., Weber, B., Huffman, J. A., Pöhlker, C., Andreae, M. O., Lang-Yona, N., Burrows, S. M., Gunthe, S. S., Elbert, W., Su, H., Hoor, P., Thines, E., Hoffmann, T., Després, V. R., and Pöschl, U.: Bioaerosols in the Earth system: Climate, health, and ecosystem interactions, *Atmospheric Research*, 182, 346–376, <https://doi.org/10.1016/j.atmosres.2016.07.018>, 2016.
- 545 Geng, H., Ryu, J., Jung, H.-J., Chung, H., Ahn, K.-H., and Ro, C.-U.: Single-Particle Characterization of Summertime Arctic Aerosols Collected at Ny-Ålesund, Svalbard, *Environmental Science & Technology*, 44, 2348–2353, <https://doi.org/10.1021/es903268j>, 2010.
- Gierens, R., Kneifel, S., D. Shupe, M., Ebell, K., Maturilli, M., and Löhnert, U.: Low-level mixed-phase clouds in a complex Arctic environment, *Atmospheric Chemistry and Physics*, 20, 3459–3481, <https://doi.org/10.5194/acp-20-3459-2020>, 2020.
- 550 Gramlich, Y., Siegel, K., Haslett, S. L., Freitas, G., Krejci, R., Zieger, P., and Mohr, C.: Revealing the chemical characteristics of Arctic low-level cloud residuals – in situ observations from a mountain site, *Atmospheric Chemistry and Physics*, 23, 6813–6834, <https://doi.org/10.5194/acp-23-6813-2023>, 2023.
- Hartmann, M., Adachi, K., Eppers, O., Haas, C., Herber, A., Holzinger, R., Hünerbein, A., Jäkel, E., Jentzsch, C., van Pinxteren, M., Wex, H., Willmes, S., and Stratmann, F.: Wintertime Airborne Measurements of Ice Nucleating Particles in the High Arctic: A Hint to a Marine, Biogenic Source for Ice Nucleating Particles, *Geophysical Research Letters*, 47, <https://doi.org/10.1029/2020GL087770>, 2020.
- 555 Huffman, J. A., Perring, A. E., Savage, N. J., Clot, B., Crouzy, B., Tummon, F., Shoshanim, O., Damit, B., Schneider, J., Sivaprakasam, V., Zawadowicz, M. A., Crawford, I., Gallagher, M., Topping, D., Doughty, D. C., Hill, S. C., and Pan, Y.: Real-time sensing of bioaerosols: Review and current perspectives, *Aerosol Science and Technology*, 54, 465–495, <https://doi.org/10.1080/02786826.2019.1664724>, 2020.
- Illingworth, A. J., Hogan, R. J., O’Connor, E. J., Bouniol, D., Brooks, M. E., Delanoë, J., Donovan, D. P., Eastment, J. D., Gaussiat, N., 560 Goddard, J. W., Haeffelin, M., Klein Baltinik, H., Krasnov, O. A., Pelon, J., Piriou, J. M., Protat, A., Russchenberg, H. W., Seifert, A., Tompkins, A. M., van Zadelhoff, G. J., Vinit, F., Willen, U., Wilson, D. R., and Wrench, C. L.: Cloudnet: Continuous evaluation of cloud profiles in seven operational models using ground-based observations, *Bulletin of the American Meteorological Society*, 88, 883–898, <https://doi.org/10.1175/BAMS-88-6-883>, 2007.
- Joly, M., Attard, E., Sancelme, M., Deguillaume, L., Guilbaud, C., Morris, C. E., Amato, P., and Delort, A. M.: Ice nucleation activity of bacteria isolated from cloud water, *Atmospheric Environment*, 70, 392–400, <https://doi.org/10.1016/j.atmosenv.2013.01.027>, 2013.
- 565 Kanji, Z. A., Ladino, L. A., Wex, H., Boose, Y., Burkert-Kohn, M., Cziczo, D. J., and Krämer, M.: Overview of Ice Nucleating Particles, *Meteorological Monographs*, 58, 1–1, <https://doi.org/10.1175/amsmonographs-d-16-0006.1>, 2017.
- Karlsson, L., Krejci, R., Koike, M., Ebell, K., and Zieger, P.: A long-term study of cloud residuals from low-level Arctic clouds, *Atmospheric Chemistry and Physics*, 21, 8933–8959, <https://doi.org/10.5194/acp-21-8933-2021>, 2021.
- 570 Karlsson, L., Baccarini, A., Duplessis, P., Baumgardner, D., Brooks, I. M., Chang, R. Y., Dada, L., Dällenbach, K. R., Heikkinen, L., Krejci, R., Leaitch, W. R., Leck, C., Partridge, D. G., Salter, M. E., Wernli, H., Wheeler, M. J., Schmale, J., and Zieger, P.: Physical and Chemical Properties of Cloud Droplet Residuals and Aerosol Particles During the Arctic Ocean 2018 Expedition, *Journal of Geophysical Research: Atmospheres*, 127, 1–20, <https://doi.org/10.1029/2021JD036383>, 2022.
- Kay, J. E., L’Ecuyer, T., Chepfer, H., Loeb, N., Morrison, A., and Cesana, G.: Recent Advances in Arctic Cloud and Climate Research, 575 <https://doi.org/10.1007/s40641-016-0051-9>, 2016.

- Khaled, A., Zhang, M., Amato, P., Delort, A. M., and Ervens, B.: Biodegradation by bacteria in clouds: An underestimated sink for some organics in the atmospheric multiphase system, *Atmospheric Chemistry and Physics*, 21, 3123–3141, <https://doi.org/10.5194/acp-21-3123-2021>, 2021.
- 580 Kopec, B. G., Feng, X., Michel, F. A., and Posmentier, E. S.: Influence of sea ice on Arctic precipitation, *Proceedings of the National Academy of Sciences*, 113, 46–51, <https://doi.org/10.1073/pnas.1504633113>, 2016.
- Korolev, A. V., Isaac, G. A., Cober, S. G., Strapp, J. W., and Hallett, J.: Microphysical characterization of mixed-phase clouds, *Quarterly Journal of the Royal Meteorological Society*, 129, 39–65, <https://doi.org/10.1256/qj.01.204>, 2003.
- Lensky, I. M. and Rosenfeld, D.: Satellite-based insights into precipitation formation processes in continental and maritime convective clouds at nighttime, *Journal of Applied Meteorology*, 42, 1227–1233, [https://doi.org/10.1175/1520-0450\(2003\)042<1227:SIIPFP>2.0.CO;2](https://doi.org/10.1175/1520-0450(2003)042<1227:SIIPFP>2.0.CO;2),  
585 2003.
- Lohmann, U., Lüönd, F., and Mahrt, F.: *An Introduction to Clouds: From the Microscale to Climate*, Cambridge University Press, Cambridge, [https://doi.org/DOI: 10.1017/CBO9781139087513](https://doi.org/DOI:10.1017/CBO9781139087513), 2016.
- Maturilli, M.: High resolution radiosonde measurements from station Ny-Ålesund (2017-04 et seq), <https://doi.org/10.1594/PANGAEA.914973>, 2020.
- 590 Maturilli, M. and Ebell, K.: Twenty-five years of cloud base height measurements by ceilometer in Ny-Ålesund, Svalbard, *Earth System Science Data*, 10, 1451–1456, <https://doi.org/10.5194/essd-10-1451-2018>, 2018.
- Matus, A. V. and L'Ecuyer, T. S.: The role of cloud phase in Earth's radiation budget, *Journal of Geophysical Research*, 122, 2559–2578, <https://doi.org/10.1002/2016JD025951>, 2017.
- Meinander, O., Dagsson-Waldhauserova, P., Amosov, P., Aseyeva, E., Atkins, C., Baklanov, A., Baldo, C., Barr, S. L., Barzycka, B., Ben-  
595 ning, L. G., Cvetkovic, B., Enchilik, P., Frolov, D., Gassó, S., Kandler, K., Kasimov, N., Kavan, J., King, J., Koroleva, T., Krupskaya, V., Kulmala, M., Kusiak, M., Lappalainen, H. K., Laska, M., Lasne, J., Lewandowski, M., Luks, B., Mcquaid, J. B., Moroni, B., Murray, B., Möhler, O., Nawrot, A., Nickovic, S., O'Neill, N. T., Pejanovic, G., Popovicheva, O., Ranjbar, K., Romanias, M., Samonova, O., Sanchez-Marroquin, A., Schepanski, K., Semenov, I., Sharapova, A., Shevnina, E., Shi, Z., Sofiev, M., Thevenet, F., Thorsteinsson, T., Timofeev, M., Umo, N. S., Uppstu, A., Urupina, D., Varga, G., Werner, T., Arnalds, O., and Vukovic Vimic, A.: Newly identified climatically and environmentally significant high-latitude dust sources, *Atmospheric Chemistry and Physics*, 22, 11 889–11 930, <https://doi.org/10.5194/acp-22-11889-2022>, 2022.
- 600 Merlivat, L. and Jouzel, J.: Global climatic interpretation of the deuterium-oxygen 18 relationship for precipitation, *Journal of Geophysical Research: Oceans*, 84, 5029–5033, <https://doi.org/10.1029/JC084iC08p05029>, 1979.
- Mioche, G., Jourdan, O., Ceccaldi, M., and Delanoë, J.: Variability of mixed-phase clouds in the Arctic with a focus on the Svalbard region: A study based on spaceborne active remote sensing, *Atmospheric Chemistry and Physics*, 15, 2445–2461, <https://doi.org/10.5194/acp-15-2445-2015>, 2015.
- Morrison, H., De Boer, G., Feingold, G., Harrington, J., Shupe, M. D., and Sulia, K.: Resilience of persistent Arctic mixed-phase clouds, *Nature Geoscience*, 5, 11–17, <https://doi.org/10.1038/ngeo1332>, 2012.
- Nomokonova, T., Ebell, K., Löhnert, U., Maturilli, M., Ritter, C., and O'Connor, E.: Statistics on clouds and their relation to thermodynamic conditions at Ny-Ålesund using ground-based sensor synergy, *Atmospheric Chemistry and Physics*, 19, 4105–4126, <https://doi.org/10.5194/acp-19-4105-2019>, 2019.
- 610 Nomokonova, T., Ebell, K., Löhnert, U., Maturilli, M., and Ritter, C.: The influence of water vapor anomalies on clouds and their radiative effect at Ny-Ålesund, *Atmospheric Chemistry and Physics*, 20, 5157–5173, <https://doi.org/10.5194/acp-20-5157-2020>, 2020.

- Noone, D., Galewsky, J., Sharp, Z. D., Worden, J., Barnes, J., Baer, D., Bailey, A., Brown, D. P., Christensen, L., Crosson, E., Dong, F.,  
615 Hurley, J. V., Johnson, L. R., Strong, M., Toohey, D., Van Pelt, A., and Wright, J. S.: Properties of air mass mixing and humidity in the  
subtropics from measurements of the D/H isotope ratio of water vapor at the Mauna Loa Observatory, *Journal of Geophysical Research  
Atmospheres*, 116, <https://doi.org/10.1029/2011JD015773>, 2011.
- Noone, K. J., Ogren, J. A., Heintzenberg, J., Charlson, R. J., and Covert, D. S.: Design and calibration of a counter-  
flow virtual impactor for sampling of atmospheric fog and cloud droplets, *Aerosol Science and Technology*, 8, 235–244,  
620 <https://doi.org/10.1080/02786828808959186>, 1988.
- Pasquier, J. T., David, R. O., Freitas, G., Gierens, R., Gramlich, Y., Haslett, S., Li, G., Schäfer, B., Siegel, K., Wieder, J., Adachi, K., Belosi,  
F., Carlsen, T., Decesari, S., Ebell, K., Gilardoni, S., Gysel-Beer, M., Henneberger, J., Inoue, J., Kanji, Z. A., Koike, M., Kondo, Y.,  
Krejci, R., Lohmann, U., Maturilli, M., Mazzolla, M., Modini, R., Mohr, C., Motos, G., Nenes, A., Nicosia, A., Ohata, S., Paglione, M.,  
Park, S., Pileci, R. E., Ramelli, F., Rinaldi, M., Ritter, C., Sato, K., Storelvmo, T., Tobo, Y., Traversi, R., Viola, A., and Zieger, P.: The  
625 Ny-Ålesund Aerosol Cloud Experiment (NASCENT) Overview and First Results, *Bulletin of the American Meteorological Society*, 103,  
E2533–E2558, <https://doi.org/10.1175/BAMS-D-21-0034.1>, 2022.
- Pedersen, C.: Zeppelin Webcam Time Series [Data set], 2013.
- Pereira Freitas, G., Adachi, K., Conen, F., Heslin-Rees, D., Krejci, R., Tobo, Y., Yttri, K. E., and Zieger, P.: Regionally sourced bioaerosols  
drive high-temperature ice nucleating particles in the Arctic, *Nature Communications*, 14, 5997, [https://doi.org/10.1038/s41467-023-  
41696-7](https://doi.org/10.1038/s41467-023-<br/>630 41696-7), 2023.
- Pöhlker, C., Huffman, J. A., and Pöschl, U.: Autofluorescence of atmospheric bioaerosols - Fluorescent biomolecules and potential interfer-  
ences, *Atmospheric Measurement Techniques*, 5, 37–71, <https://doi.org/10.5194/amt-5-37-2012>, 2012.
- Porter, G. C., Adams, M. P., Brooks, I. M., Ickes, L., Karlsson, L., Leck, C., Salter, M. E., Schmale, J., Siegel, K., Sikora, S. N., Tarn, M. D.,  
Vüllers, J., Wernli, H., Zieger, P., Zinke, J., and Murray, B. J.: Highly Active Ice-Nucleating Particles at the Summer North Pole, *Journal  
635 of Geophysical Research: Atmospheres*, 127, 1–18, <https://doi.org/10.1029/2021JD036059>, 2022.
- Prenni, A. J., Harrington, J. Y., Tjernström, M., DeMott, P. J., Avramov, A., Long, C. N., Kreidenweis, S. M., Olsson, P. Q., and Verlinde, J.:  
Can ice-nucleating aerosols affect arctic seasonal climate?, *Bulletin of the American Meteorological Society*, 88, 541–550, 2007.
- Pummer, B. G., Budke, C., Augustin-Bauditz, S., Niedermeier, D., Felgitsch, L., Kampf, C. J., Huber, R. G., Liedl, K. R., Loerting, T.,  
Moschen, T., Schauerperl, M., Tollinger, M., Morris, C. E., Wex, H., Grothe, H., Pöschl, U., Koop, T., and Fröhlich-Nowoisky, J.: Ice  
640 nucleation by water-soluble macromolecules, *Atmospheric Chemistry and Physics*, 15, 4077–4091, [https://doi.org/10.5194/acp-15-4077-  
2015](https://doi.org/10.5194/acp-15-4077-<br/>2015), 2015.
- Rantanen, M., Karpechko, A. Y., Lipponen, A., Nordling, K., Hyvärinen, O., Ruosteenoja, K., Vihma, T., and Laaksonen, A.:  
The Arctic has warmed nearly four times faster than the globe since 1979, *Communications Earth and Environment*, 3, 1–10,  
<https://doi.org/10.1038/s43247-022-00498-3>, 2022.
- 645 Rose, T., Crewell, S., Löhnert, U., and Simmer, C.: A network suitable microwave radiometer for operational monitoring of the cloudy  
atmosphere, *Atmospheric Research*, 75, 183–200, <https://doi.org/10.1016/j.atmosres.2004.12.005>, 2005.
- Ruske, S., Topping, D. O., Foot, V. E., Kaye, P. H., Stanley, W. R., Crawford, I., Morse, A. P., and Gallagher, M. W.: Evaluation of ma-  
chine learning algorithms for classification of primary biological aerosol using a new UV-LIF spectrometer, *Atmospheric Measurement  
Techniques*, 10, 695–708, <https://doi.org/10.5194/amt-10-695-2017>, 2017.



- 650 Šantl-Temkiv, T., Lange, R., Beddows, D., Rauter, U., Pilgaard, S., Dall'osto, M., Gunde-Cimerman, N., Massling, A., and Wex, H.: Biogenic Sources of Ice Nucleating Particles at the High Arctic Site Villum Research Station, *Environmental Science and Technology*, 53, 10580–10590, <https://doi.org/10.1021/acs.est.9b00991>, 2019.
- Sattler, B., Puxbaum, H., and Psenner, R.: Bacterial growth in supercooled cloud droplets, *Geophysical Research Letters*, 28, 239–242, <https://doi.org/10.1029/2000GL011684>, 2001.
- 655 Schmale, J., Zieger, P., and Ekman, A. M.: Aerosols in current and future Arctic climate, *Nature Climate Change*, 11, 95–105, <https://doi.org/10.1038/s41558-020-00969-5>, 2021.
- Sharma, S., Andrews, E., Barrie, L. A., Ogren, J. A., and Lavoué, D.: Variations and sources of the equivalent black carbon in the high Arctic revealed by long-term observations at Alert and Barrow: 1989-2003, *Journal of Geophysical Research Atmospheres*, 111, <https://doi.org/10.1029/2005JD006581>, 2006.
- 660 Shi, Y., Liu, X., Wu, M., Zhao, X., Ke, Z., and Brown, H.: Relative importance of high-latitude local and long-range-transported dust for Arctic ice-nucleating particles and impacts on Arctic mixed-phase clouds, *Atmospheric Chemistry and Physics*, 22, 2909–2935, <https://doi.org/10.5194/acp-22-2909-2022>, 2022.
- Shingler, T., Dey, S., Sorooshian, A., Brechtel, F. J., Wang, Z., Metcalf, A., Coggon, M., Mülmenstädt, J., Russell, L. M., Jonsson, H. H., and Seinfeld, J. H.: Characterisation and airborne deployment of a new counterflow virtual impactor inlet, *Atmospheric Measurement*
- 665 *Techniques*, 5, 1259–1269, <https://doi.org/10.5194/amt-5-1259-2012>, 2012.
- Shupe, M. D., Rex, M., Blomquist, B., G. Persson, P. O., Schmale, J., Uttal, T., Althausen, D., Angot, H., Archer, S., Bariteau, L., Beck, I., Bilberry, J., Bucci, S., Buck, C., Boyer, M., Brasseur, Z., Brooks, I. M., Calmer, R., Cassano, J., Castro, V., Chu, D., Costa, D., Cox, C. J., Creamean, J., Crewell, S., Dahlke, S., Damm, E., de Boer, G., Deckelmann, H., Dethloff, K., Dütsch, M., Ebell, K., Ehrlich, A., Ellis, J., Engelmann, R., Fong, A. A., Frey, M. M., Gallagher, M. R., Ganzeveld, L., Gradinger, R., Graeser, J., Greenamyre, V., Griesche, H.,
- 670 Griffiths, S., Hamilton, J., Heinemann, G., Helmig, D., Herber, A., Heuzé, C., Hofer, J., Houchens, T., Howard, D., Inoue, J., Jacobi, H. W., Jaiser, R., Jokinen, T., Jourdan, O., Jozef, G., King, W., Kirchaessner, A., Klingebiel, M., Krassovski, M., Krumpfen, T., Lampert, A., Landing, W., Laurila, T., Lawrence, D., Lonardi, M., Loose, B., Lüpkes, C., Maahn, M., Macke, A., Maslowski, W., Marsay, C., Maturilli, M., Mech, M., Morris, S., Moser, M., Nicolaus, M., Ortega, P., Osborn, J., Pätzold, F., Perovich, D. K., Petäjä, T., Pilz, C., Pirazzini, R., Posman, K., Powers, H., Pratt, K. A., Preußner, A., Quéléver, L., Radenz, M., Rabe, B., Rinke, A., Sachs, T., Schulz, A., Siebert, H.,
- 675 Silva, T., Solomon, A., Sommerfeld, A., Spreen, G., Stephens, M., Stohl, A., Svensson, G., Uin, J., Viegas, J., Voigt, C., von der Gathen, P., Wehner, B., Welker, J. M., Wendisch, M., Werner, M., Xie, Z. Q., and Yue, F.: Overview of the MOSAiC expedition- Atmosphere, <https://doi.org/10.1525/elementa.2021.00060>, 2022.
- Si, M., Evoy, E., Yun, J., Xi, Y., Hanna, S. J., Chivulescu, A., Rawlings, K., Veber, D., Platt, A., Kunkel, D., Hoor, P., Sharma, S., Richard Leitch, W., and Bertram, A. K.: Concentrations, composition, and sources of ice-nucleating particles in the Canadian High
- 680 Arctic during spring 2016, *Atmospheric Chemistry and Physics*, 19, 3007–3024, <https://doi.org/10.5194/acp-19-3007-2019>, 2019.
- Sjostrom, D. J. and Welker, J. M.: The influence of air mass source on the seasonal isotopic composition of precipitation, eastern USA, *Journal of Geochemical Exploration*, 102, 103–112, <https://doi.org/10.1016/j.gexplo.2009.03.001>, 2009.
- Sodemann, H., Schwierz, C., and Wernli, H.: Interannual variability of Greenland winter precipitation sources: Lagrangian moisture diagnostic and North Atlantic Oscillation influence, *Journal of Geophysical Research*, 113, D03 107, <https://doi.org/10.1029/2007JD008503>,
- 685 2008.

- Solomon, A., De Boer, G., Creamean, J. M., McComiskey, A., Shupe, M. D., Maahn, M., and Cox, C.: The relative impact of cloud condensation nuclei and ice nucleating particle concentrations on phase partitioning in Arctic mixed-phase stratocumulus clouds, *Atmospheric Chemistry and Physics*, 18, 17 047–17 059, <https://doi.org/10.5194/acp-18-17047-2018>, 2018.
- Spänkuch, D., Hellmuth, O., and Görsdorf, U.: What Is a Cloud? Toward a More Precise Definition, *Bulletin of the American Meteorological Society*, 103, E1894–E1929, <https://doi.org/https://doi.org/10.1175/BAMS-D-21-0032.1>, 2022.
- 690 Steen-Larsen, H. C., Johnsen, S. J., Masson-Delmotte, V., Stenni, B., Risi, C., Sodemann, H., Balslev-Clausen, D., Blunier, T., Dahl-Jensen, D., Ellehøj, M. D., Falourd, S., Grindsted, A., Gkinis, V., Jouzel, J., Popp, T., Sheldon, S., Simonsen, S. B., Sjolte, J., Steffensen, J. P., Sperlich, P., Sveinbjörnsdóttir, A. E., Vinther, B. M., and White, J. W.: Continuous monitoring of summer surface water vapor isotopic composition above the Greenland Ice Sheet, *Atmospheric Chemistry and Physics*, 13, 4815–4828, [https://doi.org/10.5194/acp-13-4815-](https://doi.org/10.5194/acp-13-4815-2013)
- 695 2013, 2013.
- Stein, A. F., Draxler, R. R., Rolph, G. D., Stunder, B. J., Cohen, M. D., and Ngan, F.: NOAA’s hysplit atmospheric transport and dispersion modeling system, <https://doi.org/10.1175/BAMS-D-14-00110.1>, 2015.
- Stopelli, E., Conen, F., Morris, C. E., Herrmann, E., Bukowiecki, N., and Alewell, C.: Ice nucleation active particles are efficiently removed by precipitating clouds, *Scientific Reports*, 5, <https://doi.org/10.1038/srep16433>, 2015.
- 700 Storelvmo, T.: Aerosol Effects on Climate via Mixed-Phase and Ice Clouds, *Annual Review of Earth and Planetary Sciences*, 45, 199–222, <https://doi.org/10.1146/annurev-earth-060115-012240>, 2017.
- Sze, K. C., Wex, H., Hartmann, M., Skov, H., Massling, A., Villanueva, D., and Stratmann, F.: Ice-nucleating particles in northern Greenland: Annual cycles, biological contribution and parameterizations, *Atmospheric Chemistry and Physics*, 23, 4741–4761, <https://doi.org/10.5194/acp-23-4741-2023>, 2023.
- 705 Szopa, S., Naik, V., Adhikary, B., Artaxo, P., Berntsen, T., Collins, W. D., Aas, W., Akritidis, D., Allen, R. J., Kanaya, Y., Prather, M. J., Kuo, C., Zhai, P., Pirani, A., Connors, S., Péan, C., Berger, S., Caud, N., Chen, Y., Goldfarb, L., Gomis, M., Huang, M., Leitzell, K., Lonnoy, E., Matthews, J., Maycock, T., Waterfield, T., Yelekçi, O., Yu, R., and Zhou, B.: Short-lived Climate Forcers Coordinating Lead Authors: Lead Authors: Contributing Authors: Review Editors: Chapter Scientist: to the Sixth Assessment Report of the Intergovernmental Panel on Climate Change, *Climate Change 2021: The Physical Science Basis. Contribution of Working Group I to the Sixth Assessment Report*
- 710 of the Intergovernmental Panel on Climate Change, pp. 817–922, <https://doi.org/10.1017/9781009157896.008>, 2021.
- Taylor, P. C., Boeke, R. C., Li, Y., and Thompson, W. J.: Arctic cloud annual cycle biases in climate models, *Atmospheric Chemistry and Physics*, 19, 8759–8782, <https://doi.org/10.5194/acp-19-8759-2019>, 2019.
- Tobo, Y., Prenni, A. J., Demott, P. J., Huffman, J. A., McCluskey, C. S., Tian, G., Pöhlker, C., Pöschl, U., and Kreidenweis, S. M.: Biological aerosol particles as a key determinant of ice nuclei populations in a forest ecosystem, *Journal of Geophysical Research Atmospheres*, 118,
- 715 100–10, <https://doi.org/10.1002/jgrd.50801>, 2013.
- Tobo, Y., Adachi, K., DeMott, P. J., Hill, T. C., Hamilton, D. S., Mahowald, N. M., Nagatsuka, N., Ohata, S., Uetake, J., Kondo, Y., and Koike, M.: Glacially sourced dust as a potentially significant source of ice nucleating particles, *Nature Geoscience*, 12, 253–258, <https://doi.org/10.1038/s41561-019-0314-x>, 2019.
- Urbański, J. A. and Litwicka, D.: The decline of Svalbard land-fast sea ice extent as a result of climate change, *Oceanologia*, 64, 535–545, <https://doi.org/10.1016/j.oceano.2022.03.008>, 2022.
- 720 Welker, J. M., Wookey, P. A., Parsons, A. N., Press, M. C., Callaghan, T. V., and Lee, J. A.: Leaf carbon isotope discrimination and vegetative responses of *Dryas octopetala* to temperature and water manipulations in a High Arctic polar semi-desert, Svalbard, *Oecologia*, 95, 463–469, <https://doi.org/10.1007/BF00317428>, 1993.

- Wendisch, M., Brückner, M., Crewell, S., Ehrlich, A., Notholt, J., Lüpkes, C., Macke, A., Burrows, J. P., Rinke, A., Quaas, J., Maturilli, M., Schemann, V., Shupe, M. D., Akansu, E. F., Barrientos-Velasco, C., Bärfuss, K., Blechschmidt, A. M., Block, K., Bougoudis, I., Bozem, H., Böckmann, C., Bracher, A., Bresson, H., Bretschneider, L., Buschmann, M., Chechin, D. G., Chylik, J., Dahlke, S., Deneke, H., Dethloff, K., Donth, T., Dorn, W., Dupuy, R., Ebell, K., Egerer, U., Engelmann, R., Eppers, O., Gerdes, R., Gierens, R., Gorodetskaya, I. V., Gottschalk, M., Griesche, H., Gryanik, V. M., Handorf, D., Harm-Altstädter, B., Hartmann, J., Hartmann, M., Heinold, B., Herber, A., Herrmann, H., Heygster, G., Höschel, I., Hofmann, Z., Hölemann, J., Hünerbein, A., Jafariserajehlou, S., Jäkel, E., Jacobi, C., Janout, M., Jansen, F., Jourdan, O., Jurányi, Z., Kalesse-Los, H., Kanzow, T., Käthner, R., Kliesch, L. L., Klingebiel, M., Knudsen, E. M., Kovács, T., Körtke, W., Krampe, D., Kretzschmar, J., Kreyling, D., Kulla, B., Kunkel, D., Lampert, A., Lauer, M., Lelli, L., Von Lerber, A., Linke, O., Löhnert, U., Lonardi, M., Losa, S. N., Losch, M., Maahn, M., Mech, M., Mei, L., Mertes, S., Metzner, E., Mewes, D., Michaelis, J., Mioche, G., Moser, M., Nakoudi, K., Neggers, R., Neuber, R., Nomokonova, T., Oelker, J., Papakonstantinou-Presvelou, I., Pätzold, F., Pefanis, V., Pohl, C., Van Pinxteren, M., Radovan, A., Rhein, M., Rex, M., Richter, A., Risse, N., Ritter, C., Rostosky, P., Rozanov, V. V., Donoso, E. R., Garfias, P. S., Salzmann, M., Schacht, J., Schäfer, M., Schneider, J., Schnierstein, N., Seifert, P., Seo, S., Siebert, H., Soppa, M. A., Spreen, G., Stachlewska, I. S., Stapf, J., Stratmann, F., Tegen, I., Viceto, C., Voigt, C., Vountas, M., Walbröl, A., Walter, M., Wehner, B., Wex, H., Willmes, S., Zanatta, M., and Zeppenfeld, S.: Atmospheric and Surface Processes, and Feedback Mechanisms Determining Arctic Amplification, *Bulletin of the American Meteorological Society*, 104, E208–E242, <https://doi.org/10.1175/BAMS-D-21-0218.1>, 2023.
- 740 WMO: Guide to Meteorological Instruments and Methods of Observation – WMO-N O. 8, Secretariat of the World Meteorological Organization, Geneva, Switzerland, 2008.
- Wookey, R., Robinson AN Parsons Welker, C. J., Press, M., Callaghan, T., Lee, J., Robinson, C., Callaghan MC Press, T., Parsons, A., and Welker, J.: Environmental constraints on the growth, photosynthesis and reproductive development of *Dryas octopetala* at a high Arctic polar semi-desert, Svalbard, *Oecologia*, 102, 478–489, 1995.
- 745 Xia, Z., Welker, J. M., and Winnick, M. J.: The Seasonality of Deuterium Excess in Non-Polar Precipitation, *Global Biogeochemical Cycles*, 36, 1–31, <https://doi.org/10.1029/2021GB007245>, 2022.
- Zieger, P., Fierz-Schmidhauser, R., Gysel, M., Ström, J., Henne, S., Yttri, K. E., Baltensperger, U., and Weingartner, E.: Atmospheric Chemistry and Physics Effects of relative humidity on aerosol light scattering in the Arctic, *Tech. rep.*, [www.atmos-chem-phys.net/10/3875/2010/](http://www.atmos-chem-phys.net/10/3875/2010/), 2010.
- 750 Zieger, P., Heslin-Rees, D., Karlsson, L., Koike, M., Modini, R., and Krejci, R.: Black carbon scavenging by low-level Arctic clouds, *Nature communications*, 14, 5488, <https://doi.org/10.1038/s41467-023-41221-w>, 2023.

**Table 1. Summary of detected fluorescent primary biological aerosol particles (fPBAP) inside low-level Arctic clouds.** Summer include the months from June to September, while winter refers to October ~~to~~ through May.

	fPBAP measured (#)	Number of cloud events (#)	Total hours of sampled clouds (H)	Clouds containing fPBAP (%)	fPBAP conc. (mean, $10^{-3}\text{L}^{-1}$ )	fPBAP conc. (median, $10^{-3}\text{L}^{-1}$ )	fPBAP contr. (mean, %)	fPBAP contr. (median, %)
Summer	476	156	612	67	8.1	4.8	0.032	0.012
Winter	51	53	200	45	4.3	0	0.005	0
<u>Summer</u> <u>Winter</u>	9	2.9	3.1	1.47	-	-	-	-

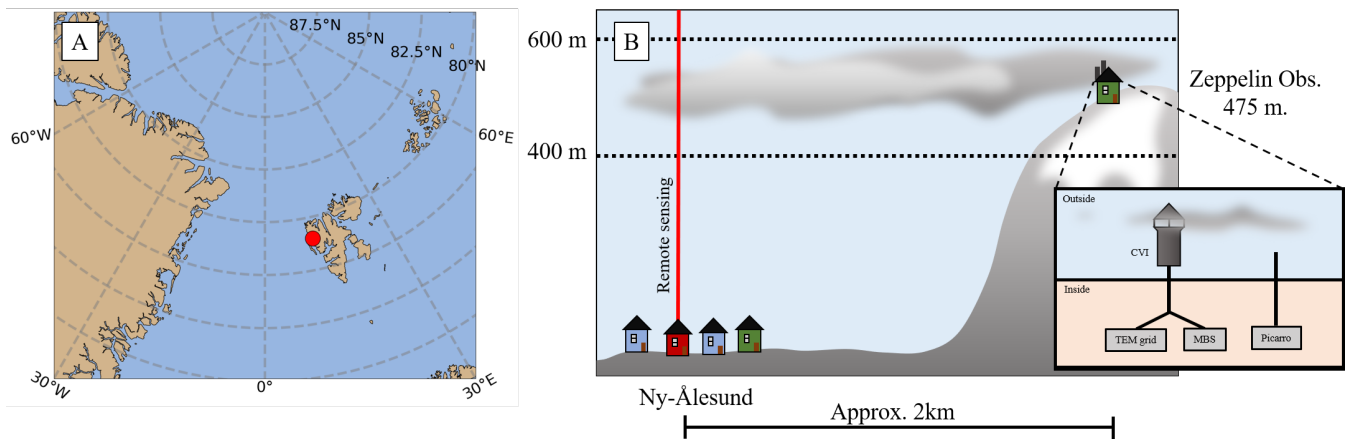


**Figure 1. Sampling location and measurement setup.** **aA)** Location of Ny-Ålesund on the Norwegian archipelago of Svalbard (red dot). **bB)** Schematic demonstrating the positioning of the different measurements in the town of Ny-Ålesund, where remote sensing took place, and at the Zeppelin Observatory (475 m asl meter above sea level), where in-situ cloud, aerosol and water vapour-vapor measurements were performed. For the cloud characterization via Cloudnet, the altitude between 400 and 600 meters was taken into account (dashed line). At the Zeppelin Observatory the transmission electron microscopy (TEM) grid sampler and the mutliparameter bioaerosol spectrometer (MBS) sampled cloud residuals from a counterflow virtual impactor (CVI) inlet. The Picarro sampled water vapour-vapor from its own gas-phase inlet.

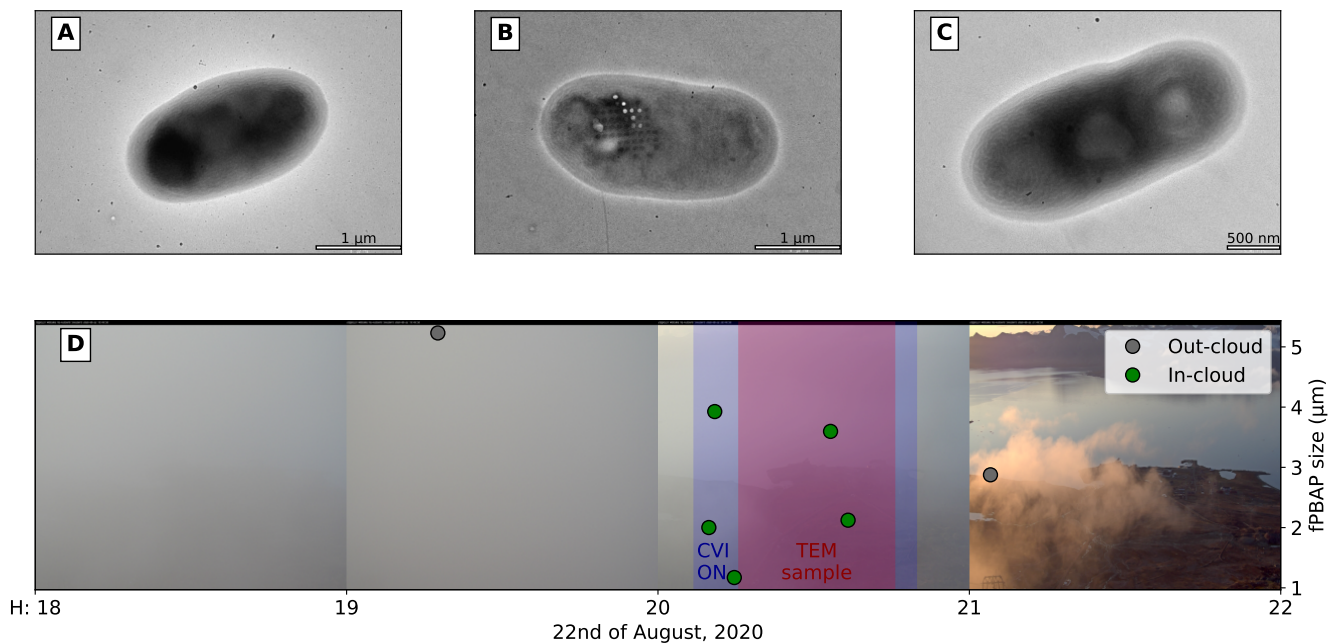


**Figure 2.** Example of PBAP within cloud residuals as identified via TEM and MBS analysis. Example of primary biological aerosol particles (PBAP) within cloud residuals as identified via transmission electron microscopy (TEM) and multiparameter bioaerosol spectrometer (MBS) analysis. Panel a-e-A-C show identified PBAP particles within-on the TEM sample taken on the 22nd of August 2020 (sampled behind-downstream of the counterflow virtual impactor, CVI, inlet). Panel d-D shows webcam images (taken from Pedersen, 2013) of the cloud event and the periods of the CVI operation (blue area) and TEM sampling (pink area)period. In addition, the fluorescent PBAP (fPBAP) particles identified by the MBS are shown in the background as a function of their size (right axis). Out-of-cloud-Out-cloud measured fPBAP (MBS sampling from the-a whole-air-inlet) are shown for context. Dots on the particle shown in panel B are due to beam damage on the particle by the electron beam induced damage.



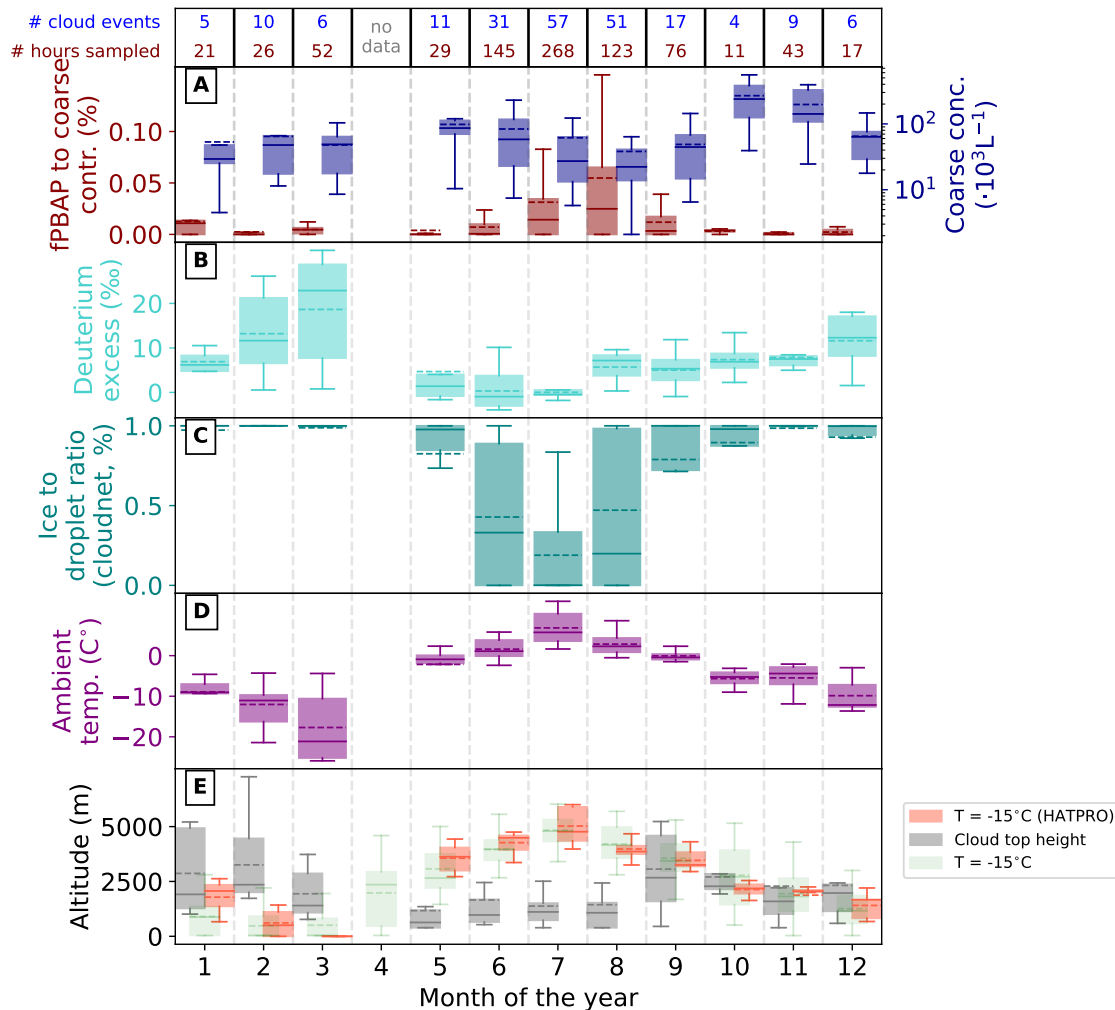


**Figure 3. Example of a mixed-phase cloud event measured in September 2020.** a) Cloudnet classification (at Annual cycles of all relevant bioaerosol, water vapor, cloud and meteorological parameters during cloud events). Above panel A, the height-number of Zeppelin-observatory cloud events (CE) and visibility (directly measured-sampled hours per month of the year. For a detailed availability of data see Table S1. These values refer to all datasets except for temperature soundings at Zeppelin-observatory) panel E. Light-blue boxes above and in A) Coarse aerosol ( $D > 0.8 \mu\text{m}$ ) concentration as measured by the panels below indicate periods where CVI sampling occurred-multiparameter bioaerosol spectrometer, along with the ice-to-droplet-ratio-contribution of each-CVI-cloud-event-calculated using the Cloudnet data. b) fluorescent primary biological aerosol particles (fPBAP) Wind direction and speed at to the coarse mode (at Zeppelin Observatory). c) Water vapor-deuterium excess and ambient temperature (d-excess, at Zeppelin Observatory). d) Fluorescent primary biological aerosol particles-Ice-to-droplet ratio, as calculated using Cloudnet data (fPBAP)-measured by above Ny-Ålesund at the multiparameter bioaerosol spectrometer height of Zeppelin Observatory). E) Ambient temperature (MBSat Zeppelin Observatory) categorized by size. Out-cloud PBAP are shown for context. Observations E) Altitude when air temperature is  $-15^\circ$  as measured by daily atmospheric soundings from panel b-d were taken 2019-06 to 2020-12 and per CE by the HATPRO measured above Ny-Ålesund at the height of Zeppelin Observatory. Furthermore, the cloud top height of the lowest cloud is also shown.

**Example of a droplet cloud event measured in July 2020.** a) Cloudnet classification (at the height of Zeppelin-observatory) and visibility (directly measured at Zeppelin observatory). Light blue boxes above and in the panels below indicate periods where CVI sampling occurred along with the ice-to-droplet ratio of each-CVI-cloud-event-calculated using the Cloudnet data. b) Wind direction and speed at the Zeppelin

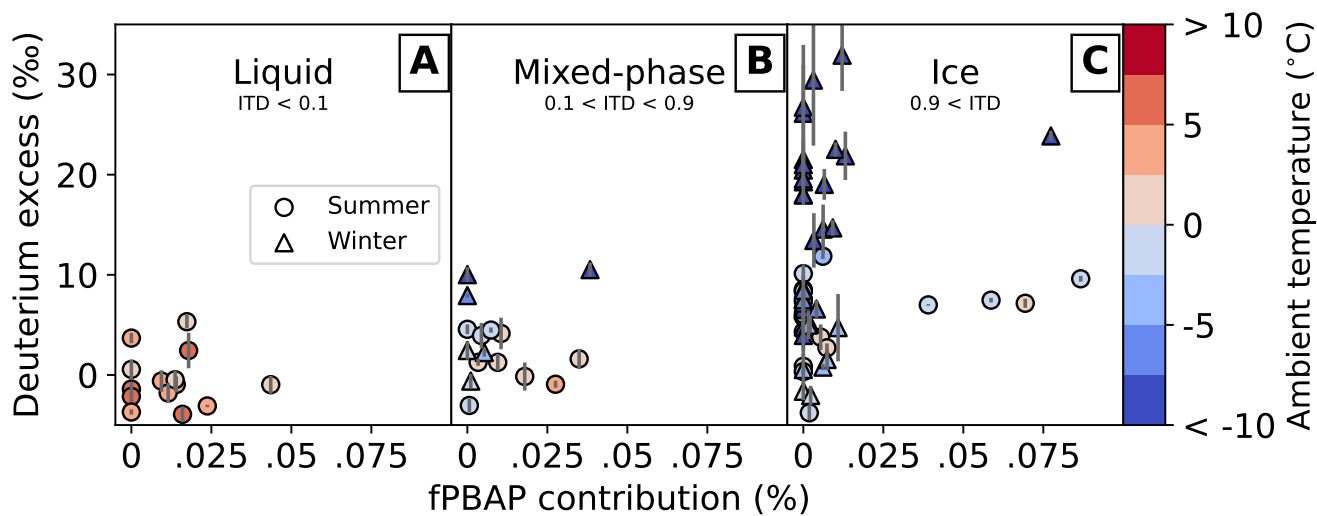


**Figure 4. Deuterium-excess vs. FPBAP contribution to aerosol coarse-mode number concentration. Deuterium excess (d-excess) vs. fluorescent primary biological aerosol particles (FPBAP) contribution to aerosol coarse-mode number concentration.** Relationship shown for **aA)** liquid, **bB)** mixed-phase and **cC)** ice cloud events as classified by the ice-to-droplet (ITD) ratio. Color-code represents the mean ambient temperature at 500-475 meters above sea level. **s.l.** Triangles denote clouds in winter while circles show summer cloud events. Individual points are arithmetic mean values and error bars represent the corresponding standard deviation of the deuterium-excess d-excess.

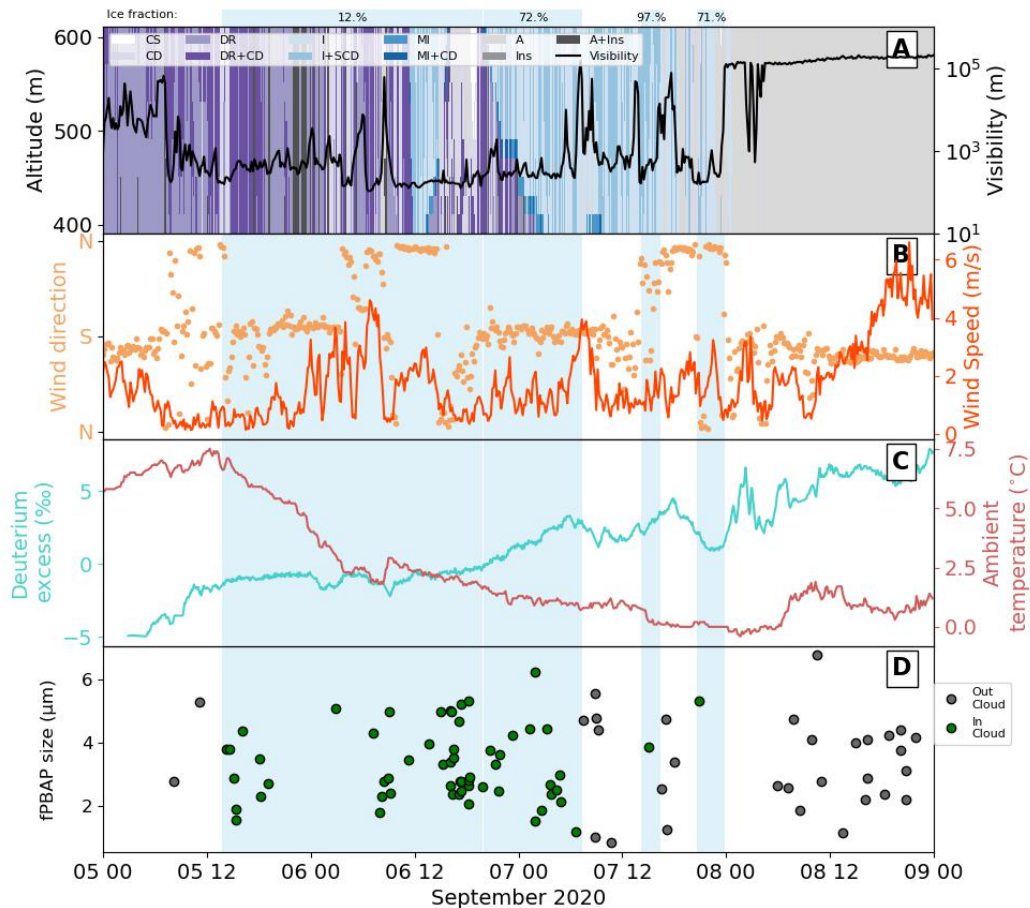


**Figure 5.** Example of a mixed-phase cloud event measured in September 2020. A) Cloudnet classification (at the height of Zeppelin Observatory) and visibility (directly measured at Zeppelin Observatory). Light blue boxes above and in the panels below indicate periods where counterflow virtual impactor (CVI) inlet sampling occurred along with the ice fraction of each CVI cloud event calculated using the Cloudnet data. B) Wind direction and speed at the Zeppelin Observatory. C) Water vapor deuterium excess and ambient temperature. D) Fluorescent primary biological aerosol particles (fpBAP) measured categorized by size. Out-cloud fpBAP are shown for context.